

Transversal parametric oscillation and its external stability in photorefractive sillenite crystals

Evgeny V. Podivilov,¹ Henrik C. Pedersen,² Per M. Johansen,³ and Boris I. Sturman⁴

¹*Institute of Automation and Electrometry, Academy of Science, Universitetskij Prospect 1, Novosibirsk, 630090, Russia*

²*School of Physical Sciences, University of Kent, Canterbury, CT2 7NR, United Kingdom*

³*Optics and Fluid Dynamics Department, Risø National Laboratory, DK-4000 Roskilde, Denmark*

⁴*International Institute for Non-Linear Studies, Siberian Branch, 630090 Novosibirsk, Russia*

(Received 27 October 1997)

We develop the nonlinear theory of transversal parametric oscillation in photorefractive sillenite crystals. The theory is nonlinear in the sense that the nonlinear feedback from the parametric space-charge field waves, above threshold of their excitation, is taken into account. In this manner, an analytical solution for the stationary state of the parametric waves is obtained. We analyze the stationary states' stability both against small perturbations in amplitude and phase (internal stability) and against excitation of new secondary waves (external stability). It is shown that the stationary state of transversal parametric oscillation is stable within certain regions of external and internal parameters. This is opposed to the degenerate case ($K/2$ subharmonic generation), which is unstable. [S1063-651X(98)07505-9]

PACS number(s): 42.40.Pa, 42.65.Hw, 42.70.Nq

I. INTRODUCTION

The parametric wave interaction is a very general phenomenon observed for many types of waves in continuous media. The interaction is known, for example, for plasma waves [1,2], spin waves [3], and optical waves [4]. One of the latest examples of parametric wave interaction is the one that takes place between so-called space-charge waves (SCWs) in photorefractive crystals of the sillenite family [$\text{Bi}_{12}\text{SiO}_{20}$, (BSO), $\text{Bi}_{12}\text{GeO}_{20}$, and $\text{Bi}_{12}\text{TiO}_{20}$]. This is the subject of the present paper.

One of the most common ways of exciting SCWs in a sillenite crystal is to apply a constant, homogeneous electric field to the crystal and then illuminate it by two intersecting coherent laser beams, as shown schematically in Fig. 1. The laser beams form a light interference pattern in the crystal and by introducing a frequency shift Ω in one of the beams the light pattern starts moving in a direction perpendicular to the light fringes. As a consequence of the photorefractive effect, this light pattern, which may be thought of as a wave of light intensity, is followed by the formation of a SCW that has the same wave vector, \vec{K} , and frequency, Ω , as the intensity pattern. This SCW is referred to as the fundamental wave. When the frequency is varied, one can observe a resonant behavior of the fundamental SCW when Ω reaches the medium's eigenfrequency [5].

In 1988 Mallick *et al.* [6] discovered a new and very spectacular phenomenon when they excited a SCW as outlined above. They found that when Ω was increased well above the eigenfrequency, the SCW lost the spatial periodicity of the driving light pattern. In the simplest case, a SCW with the spatial frequency $\vec{K}/2$ appeared in addition to the fundamental SCW with wave vector \vec{K} . By further increasing Ω the authors observed that the wave vector of the additional SCW changed from $\vec{K}/2$ to $\vec{K}/3$ and then to $\vec{K}/4$. Since the wave vectors of the additional waves appeared to be integer fractions of \vec{K} , this new effect was referred to as spatial subharmonic generation. However, in the years that fol-

lowed, the cases of $\vec{K}/2$, $\vec{K}/3$, and $\vec{K}/4$ subharmonic generation proved to be just special cases of a much wider class of phenomena which includes continuous broadening and splitting of the additional wave vectors along both the longitudinal (parallel to \vec{K}) and transversal (perpendicular to \vec{K}) directions [7–10]. The whole class of phenomena may be referred to as photorefractive parametric oscillation (PPO) [7] because of its close resemblance to the analogous optical process, optical parametric oscillation. In characterizing PPO, one can distinguish between three characteristic types that have been observed experimentally, degenerate (DPO), longitudinal (LPO), and transversal (TPO) parametric oscillation [10]. The wave vector schemes of the three types are illustrated in Fig. 2.

The origin of PPO became clear a few years ago [11–13]. It turned out that parametric excitation of weakly damped low-frequency eigenmodes of the medium—parametric SCWs [14,15]—lies in its basis. The existence of such modes in the sillenite crystals is due to a large value of the lifetime-mobility product for photoelectrons. This gives rise to a large drift length of the photoelectrons and, consequently, a large quality factor of the SCWs, see, e.g., [11]. As the threshold of the instability leading to PPO decreases with an increasing quality factor, the SCWs are easiest excited when the lifetime-mobility product is large. The para-

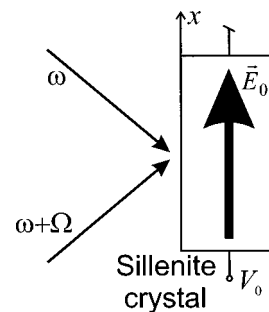


FIG. 1. Schematic diagram of the basic configuration for exciting space-charge waves in a photorefractive sillenite crystal.

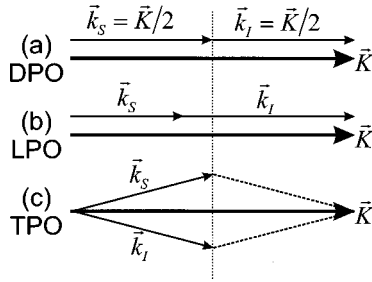


FIG. 2. Geometrical scheme of the wave vectors for the three characteristic types of PPO. \vec{k}_s and \vec{k}_l are the wave vectors of the additional SCWs and \vec{K} is the fundamental wave vector. The cases (a), (b), and (c) are related to the cases of degenerate parametric oscillation (DPO), longitudinal parametric oscillation (LPO), and transversal parametric oscillation (TPO), respectively.

metric resonance conditions are provided either by frequency detuned light waves [6,16–18] (running grating technique) or by an alternating applied electric field [19–22]. The theory of parametric excitation of the eigenmodes, linear in their amplitudes, enabled one to explain a number of characteristic features of PPO [13,23,24].

Along with the origin of PPO, its relation to the photorefractive effect also became clear. The photorefractive effect is described by two wave equations: the material wave equation, which governs the SCWs, and the optical wave equation which governs the light propagation. Basically, PPO is a material effect, hence, it is described by the material wave equation. So, as regards PPO, the optical part of the photorefractive effect is in use solely when visualizing the effect experimentally, as the induced SCWs are read out by diffraction of an optical read-out beam. Unfortunately, the material and optical effects are mixed in many of the PPO experiments performed [6–10,16–19]. However, in 1994 McClelland *et al.* [12] introduced an experimental configuration in which it is possible to isolate the two effects from one another due to which more “pure” results can be obtained. It was then finally proven that, basically, PPO is a nonlinear material effect that can appear independently of the optical effect.

The linear theory of PPO [11] is only a first step towards a full description of the process, as this theory only describes the growth rate of the parametric wave amplitudes and the threshold values of different parameters. It does not incorporate the effect of saturation (steady state) of the parametric wave amplitudes nor does it touch the problem of stability against excitation of new parametric waves. To describe these important aspects one needs to develop a nonlinear theory which involves the parametric waves’ nonlinear interaction with themselves and other waves present in the medium. The necessity for such a theory is obvious not only because of completeness, but also in view of the fact that nearly all experimental results on PPO have been obtained in steady state.

The foundations of the nonlinear theory were laid in Ref. [22] in which the steady state of the simplest case, $\vec{K}/2$ subharmonic generation (DPO), was analyzed. It was shown that the amplitudes of the saturating parametric waves are determined to a large degree by their nonlinear frequency shifts. In particular, various stationary states of the parametric

waves beyond the threshold as well as their feedback to the fundamental wave may be expressed in terms of these shifts. Another important notion of the nonlinear theory is the renormalization of the nonlinear coupling constant. Such a renormalization is important for analyzing the stability of the nonlinear regimes against small perturbations. As was shown in Ref. [22], the $\vec{K}/2$ subharmonic state is always unstable with respect to excitation of parametric waves with wave vectors near $\vec{K}/2$ (so-called modulational instability).

So, until now, the only knowledge we have as regards the steady state of PPO is that the simplest case, $\vec{K}/2$ subharmonic generation, is unstable. In this paper we wish to extend the analysis of Ref. [22] to include a general state of TPO, i.e., a general transversal split between the parametric wave vectors is allowed. The reason for choosing TPO and not LPO is that the theoretical treatment of the latter is more complicated if one wants to describe the entire range of longitudinal split. Moreover, the TPO case is still the most spectacular one, as its origin is still not completely understood. We start our analysis in Sec. II by considering the fundamental relations connected with generation of SCWs, such as the wave equation and the dispersion law for eigenwaves. Based on the wave equation we introduce two nonlinear coupling coefficients, which simplifies the derivation of the nonlinear theory. In Sec. III we present the linear analysis of the stability of the fundamental wave against excitation of parametric waves. In this section the main characteristics of parametric waves are explained and the use of our nonlinear coupling coefficients is demonstrated. In Sec. IV we present the main ideas of the nonlinear theory and introduce the concept of nonlinear frequency shift. In Sec. V the steady states of the parametric waves are found from the nonlinear theory and in Sec. VI the stability of these steady state solutions is analyzed against small perturbations in the steady state amplitudes. This is referred to as analysis of internal stability. The stability analysis is then extended in Sec. VII to the external type in which the perturbations assume the form of new parametric waves. This analysis leads us to Sec. VIII in which the main results are discussed.

II. FUNDAMENTAL RELATIONS

In this section we describe the fundamental characteristics of SCWs in sillenite crystals. We consider here, as we do throughout the paper, an experimental configuration like the one shown in Fig. 1. Two coherent optical beams are incident symmetrically to a photorefractive sillenite crystal so that the applied electric field \vec{E}_0 and the wave vector of the light interference pattern, \vec{K} , are both directed along the x axis. Due to the frequency shift Ω the light interference pattern I moves as a harmonic intensity wave along the x axis, thus its dependence on time and space can be written in the following form:

$$I = I_0 + I_1 = I_0 [1 + m \cos(Kx - \Omega t)], \quad (1)$$

where I_0 and I_1 are the dc and ac parts of the intensity, m is the intensity contrast, and K is the magnitude of \vec{K} . Due to the photoconductivity of the crystal the light excites electrons from filled donors to the conduction band after which

they are free to drift and diffuse away from the light regions, in which many electrons are excited, to darker regions where they can recombine with empty donor sites. This results in an inhomogeneous charge distribution which moves along with the light pattern, hence, a space-charge wave is formed. The photoexcitation, drift, diffusion, and recombination of electrons are described by the band transport equations whereas the Poisson equation governs the space-charge field \vec{E}_1 generated by the charge separation [25]. Applied to crystals of the sillenite family, all these equations can be combined to give one single equation for the space-charge field [7,10,11]:

$$\begin{aligned} & \dot{\vec{E}}_0 \cdot (\nabla^2 \dot{\vec{E}}_1) + \frac{k_B T}{q} \vec{\nabla} \cdot (\nabla^2 \dot{\vec{E}}_1) - \frac{1}{\mu \tau} \vec{\nabla} \cdot \dot{\vec{E}}_1 - \zeta I_0 \vec{\nabla} \cdot \dot{\vec{E}}_1 \\ & + \frac{k_B T}{q} \omega_0 \vec{\nabla} \cdot (\nabla^2 \vec{E}_1) + \omega_0 \vec{E}_0 \cdot (\nabla^2 \vec{E}_1) \\ & = \zeta \vec{E}_0 \cdot (\vec{\nabla} I_1) + \frac{k_B T}{q} \zeta \nabla^2 I_1 + \underline{\underline{\zeta \vec{\nabla} \cdot (I_1 \vec{E}_1)}} \\ & - \underline{\underline{\vec{\nabla} \cdot [\vec{E}_1 (\vec{\nabla} \cdot \dot{\vec{E}}_1)]}}. \end{aligned} \quad (2)$$

This is referred to as the material wave equation. Note that one nonlinear term which was included for completeness in Refs. [7,10] has been omitted here because it gives only minor contributions to the final results. k_B is here the Boltzmann constant, T is the absolute temperature, q is the absolute value of the electronic charge, μ is the mobility of free electrons, and τ is the free electron lifetime. The parameters ω_0 and ζ are given by $\omega_0 = s I_0 N_D / N_A$ and $\zeta = s q N_D / \epsilon_0 \epsilon_S$ where s is the cross section of the photoexcitation of electrons, N_D is the density of donors, N_A is the density of acceptors, and $\epsilon_0 \epsilon_S$ is the permittivity of the crystal. The dot above some terms in Eq. (2) denotes the time derivative. In deriving the wave equation it has been assumed that the space-charge field is much less than the so-called saturation field given by $E_{\text{sat}} = q N_A / \epsilon_0 \epsilon_S K$ [26]. This condition is always fulfilled for the relatively small wave numbers involved in the PPO processes. The details of the derivation of Eq. (2) can be found in Refs. [7,11].

The left-hand side of Eq. (2) is linear in \vec{E}_1 ; it determines the fundamental characteristics of the eigenwaves to be presented in Sec. II B. The first two terms on the right-hand side represent the driving force due to the intensity distribution I_1 . The two doubly underlined terms on the right-hand side of Eq. (2) are referred to as nonlinear terms. The first term is a so-called parametric term in the sense that the coefficient I_1 oscillates harmonically. The parametric term can cause nonlinear coupling between the intensity wave I_1 and the space-charge field wave \vec{E}_1 . The second doubly underlined term describes the eigennonlinearity. This term is responsible for the space-charge field's interaction with itself. The reason why both doubly underlined terms can be referred to as nonlinear is that they both give rise to nonlinear effects, such as higher harmonic generation and parametric oscillation.

As mentioned, Eq. (2) describes the wave propagation of the space-charge field. There exist, however, other equivalent waves in the crystal that in temporal and spatial structure exactly mimic the space-charge field waves. First, the space-

charge field waves are formed by space-charge waves; they are connected simply by the Poisson equation. Secondly, one could also choose to consider the waves of the electrostatic potential φ given by $\vec{E}_1 = -\vec{\nabla} \varphi$. This approach has been used before [11,22]. Finally, because photorefractive media exhibit Pockels effect the space-charge field waves are accompanied by waves in the permittivity of the crystal which can be referred to as holographic waves or running phase gratings. However, because all the equivalent waves are connected by simple, linear relations we need only choose one of them to describe the wave propagation. In this paper, we choose from now on the space-charge field waves (SCFWs) described by Eq. (2), as this parameter is the one typically considered in photorefractive science.

A. Linear eigenwaves

Before describing the nonlinear processes it is convenient to consider first the linear case. This is because the waves that take part in the nonlinear interactions appear to have spatial and temporal characteristics similar to those for the linear eigenwaves. How can we excite an eigenwave? Let us consider the experimental configuration shown in Fig. 1, where, provisionally, the light pattern is characterized by an arbitrary wave vector \vec{k} that is not necessarily directed along the x axis. The light pattern is assumed to have a sufficiently low contrast m so we can assume that the medium responds linearly by forming a SCFW with the same wave vector and temporal frequency (\vec{k} and Ω) as the driving light pattern. Then, after some time, steady state is reached, i.e., a SCFW with constant amplitude is present. After that we suddenly switch off the light contrast. In practice, this can be done, for example, by a rapid sine-form phase modulation of one of the optical beams [27]. In this case the ac part of the light pattern disappears and, thus, the driving force equals zero. The question is then, how will the SCFW decay in this situation? The answer is, it will decay as an eigenwave, also sometimes called a free wave as the wave is not forced by any external force.

To analyze this formally we insert an *Ansatz* for the wave, $\vec{E}_1 = \hat{k} E_{10} \exp(i\vec{k} \cdot \vec{r} - i\omega t) + \text{c.c.}$, into the linear, undriven version of the wave equation (2), i.e., the right-hand side is set equal to zero. Here \hat{k} is a unit vector along \vec{k} , E_{10} is the initial amplitude of the space-charge field, ω is the (unknown) frequency, and ‘‘c.c.’’ stands for complex conjugate. To obtain nontrivial solutions, we find that ω and \vec{k} have to fulfill the following so-called linear dispersion relation:

$$\omega = \omega_0 \frac{E_{q,\vec{k}} + E_{D,\vec{k}} - i E_0}{E_0 + i E_{D,\vec{k}} + i E_{M,\vec{k}}} \equiv \bar{\omega}_{\vec{k}} - i \gamma_{\vec{k}}, \quad (3)$$

where $E_{q,\vec{k}} = q N_A / \epsilon_0 \epsilon_S k_x$, $E_{D,\vec{k}} = k_B T k^2 / q k_x$, and $E_{M,\vec{k}} = (\mu \tau k_x)^{-1}$ are characteristic electric fields. k_x denotes the x component (longitudinal component) of \vec{k} . $\bar{\omega}_{\vec{k}}$ is referred to as the eigenfrequency and $\gamma_{\vec{k}}$ is called the damping coefficient of the eigenwave. In conclusion, the space-charge field wave decays as an eigenwave with the frequency $\bar{\omega}_{\vec{k}}$ and the damping coefficient $\gamma_{\vec{k}}$.

By taking the imaginary part of Eq. (3) one finds that three terms contribute to the damping of the waves: one due

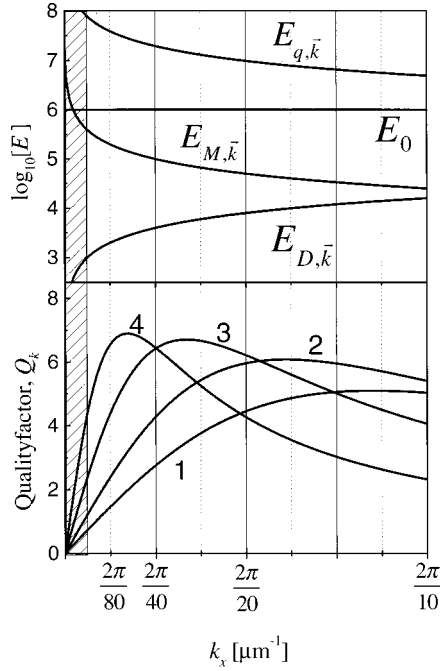


FIG. 3. Dependence of the characteristic fields $E_{q,\vec{k}}$, $E_{M,\vec{k}}$, and $E_{D,\vec{k}}$ on a \log_{10} scale (upper plot) and the quality factor $Q_{\vec{k}}$ (lower plot) on the longitudinal component of the wave vector, k_x . In the lower plot curves 1–4 correspond to $E_0=1, 5, 10,$ and 20 kV/cm, respectively. All plots have been obtained on the basis of typical material parameters for the sillenite crystal BSO [7].

to diffusion, one due to drift, and one due to recombination of the electrons. Thus energy is lost as (i) Ohmic losses, when the electrons diffuse and drift through the medium and (ii) recombination losses, when the electrons jump from the high-energy conduction band level to the low-energy donor level.

As the expressions for $\bar{\omega}_{\vec{k}}$ and $\gamma_{\vec{k}}$ are rather complicated in \vec{k} we wish to introduce a few simplifications. To justify these we have plotted the different characteristic fields versus k_x in Fig. 3. We consider in this figure the interval where $0 < k_x < 2\pi/10 \mu\text{m}^{-1}$ because this is the region where the PPO processes typically take place. It is seen that if we choose E_0 to be about 10^6 V/m ($\log_{10}[E_0]=6$) we can assume that apart from the narrow, hatched region in which k_x is less than about $2\pi/150 \mu\text{m}^{-1}$ we have the following conditions fulfilled: $E_{q,\vec{k}} \gg E_0 \gg E_{M,\vec{k}}, E_{D,\vec{k}}$. In this case we have $\bar{\omega}_{\vec{k}} \approx \omega_{\vec{k}} \equiv \omega_0 E_{q,\vec{k}}/E_0$. Moreover, as $E_{D,\vec{k}}$ is small everywhere in the considered region of k_x we can neglect this field. As we shall see later, some particular subprocesses in PPO involve waves with k_x being very close to zero. In these cases we cannot set $\bar{\omega}_{\vec{k}} = \omega_{\vec{k}}$, so there we have to use the full expression.

In the lower part of Fig. 3 we have plotted the so-called quality factor $Q_{\vec{k}}$, which is given by $Q_{\vec{k}} = \bar{\omega}_{\vec{k}}/\gamma_{\vec{k}}$, for various values of E_0 . $Q_{\vec{k}}/2\pi$ expresses the number of wavelengths the free wave travels before its amplitude is down to $1/e$ of its original value. If we choose $E_0 = 10^6$ V/m it is seen that outside the hatched region the quality factor can be considered as being much larger than unity, which, as we shall see, is of major importance in the nonlinear theory to be considered in this paper. It is worth noting that if the trans-

versal component of \vec{k} is increased, the quality factor decreases. Hence, longitudinally propagating eigenwaves (i.e., $\vec{k} \parallel \vec{E}_0$) are the weakest damped modes.

B. The fundamental wave

In our analysis of PPO we also need to know the space-charge field in the forced case, i.e., when the intensity contrast is present. So, now we consider again the case where the light pattern runs along the x axis with a wave vector $\vec{K} \parallel \vec{E}_0$. We want to find the space-charge field in the linear case, hence, we neglect the nonlinear terms in Eq. (2). In this case the space-charge field has the same spatiotemporal form as the intensity pattern, i.e., $\vec{E}_1 = \hat{x} E_0 e_{\vec{K},L} \exp(iKx - i\Omega t) + \text{c.c.}$, where \hat{x} is a unit vector in the x direction. This wave is referred to as the fundamental wave. By using Eq. (2) one can obtain the following expression for the normalized amplitude, $e_{\vec{K},L}$ [5,11]:

$$e_{\vec{K},L} = \frac{m}{2} \frac{\omega_{\vec{K}}}{\Omega - \omega_{\vec{K}} + i\gamma_{\vec{K}}}, \quad (4)$$

where we assume that K is outside the hatched region in Fig. 3, thus $\bar{\omega}_{\vec{K}} \approx \omega_{\vec{K}}$. The subscript ‘‘L’’ refers to the linear case. It is known that the linear expression in Eq. (4) is only valid in restricted intervals of m and Ω . For sufficiently high values of m and for Ω sufficiently close to the fundamental eigenfrequency $\omega_{\vec{K}}$, nonlinear contributions from higher order waves affect the fundamental amplitude [28,29]. However, the PPO effects considered in this paper occur for Ω far from $\omega_{\vec{K}}$ (for $\Omega \approx 4\omega_{\vec{K}}$) due to which Eq. (4) can be used with good accuracy even for $m=1$. For this region of Ω we can even make further simplifications and write

$$e_{\vec{K},L} \equiv \frac{m}{2} \frac{\varepsilon}{1 - \varepsilon}, \quad (5)$$

where ε is a dimensionless parameter given by $\varepsilon = \omega_{\vec{K}}/\Omega$.

C. Wave equation in k space

In the nonlinear case the space-charge field involves waves with other wave vectors than the one prescribed by the intensity pattern. Hence, the space-charge field consists, in general, of a sum over all waves present in the medium, i.e.,

$$\vec{E}_1 = E_0 \sum_{\alpha} \hat{k}_{\alpha} \tilde{e}_{\vec{k}_{\alpha}} \exp(i\vec{k}_{\alpha} \cdot \vec{r}), \quad (6)$$

where α numerates the waves. $\tilde{e}_{\vec{k}_{\alpha}}$ is the normalized, complex, and time oscillating amplitude of the wave with wave vector \vec{k}_{α} . Since the space-charge field is a real quantity we have that $\tilde{e}_{-\vec{k}_{\alpha}} = -\tilde{e}_{\vec{k}_{\alpha}}^*$. By combining Eq. (6) with the wave equation (2) and singling out the terms proportional to $\exp(i\vec{k}_{\alpha} \cdot \vec{r})$ we obtain

$$\begin{aligned}
\dot{\tilde{e}}_{\vec{k}_\alpha} + (\gamma_{\vec{k}_\alpha} + i\bar{\omega}_{\vec{k}_\alpha})\tilde{e}_{\vec{k}_\alpha} &= -i \frac{m}{2} \omega_{\vec{k}_\alpha} \delta_{\alpha F} \exp(-i\Omega t) \\
&\quad - \frac{m}{2} (i\bar{\omega}_{\vec{k}_\alpha} + \gamma_{\vec{k}_\alpha}) \\
&\quad \times \left[\frac{\vec{k}_\alpha \cdot (\vec{k}_\alpha + \vec{K})}{k_\alpha |\vec{k}_\alpha + \vec{K}|} \tilde{e}_{\vec{k}_\alpha + \vec{K}} \exp(i\Omega t) \right. \\
&\quad \left. + \frac{\vec{k}_\alpha \cdot (\vec{k}_\alpha - \vec{K})}{k_\alpha |\vec{k}_\alpha - \vec{K}|} \tilde{e}_{\vec{k}_\alpha - \vec{K}} \exp(-i\Omega t) \right] \\
&\quad - \frac{\gamma_{\vec{k}_\alpha} + i\bar{\omega}_{\vec{k}_\alpha}}{i\omega_{\vec{k}_\alpha}} \sum_{\beta} \frac{(\vec{k}_\alpha \cdot \vec{k}_\beta) |\vec{k}_\alpha - \vec{k}_\beta|}{k_\alpha k_\beta k_{\alpha,x}} \\
&\quad \times \tilde{e}_{\vec{k}_\beta} \tilde{e}_{\vec{k}_\alpha - \vec{k}_\beta}, \tag{7}
\end{aligned}$$

where $\delta_{\alpha F}$ is the Kronecker delta; the index ‘‘F’’ refers to fundamental, i.e., $\vec{k}_F = \vec{K}$. Again, the sum over β includes all the waves present. The length of a vector \vec{k}_α is denoted either by k_α or by $|\vec{k}_\alpha|$ and the x component of the vector is denoted by $k_{\alpha,x}$. Equation (7) is the wave equation in \vec{k} representation; it is valid for all values of $k_{\alpha,x}$ considered in Fig. 3, i.e., also in the hatched region. As in Eq. (2) the doubly underlined terms on the right-hand side of Eq. (7) represent the parametric nonlinearity and the eigennonlinearity, respectively.

D. Nonlinear three-wave interaction

The quadratic structure of the nonlinear terms in Eq. (7) implies that, basically, it is nonlinear three-wave interactions that can take place in the cases under study. As a first example, suppose that two SCFWs, $e_{\vec{k}_\alpha} \exp(i\vec{k}_\alpha \cdot \vec{r} - i\omega_\alpha t) + \text{c.c.}$, $e_{\vec{k}_\beta} \exp(i\vec{k}_\beta \cdot \vec{r} - i\omega_\beta t) + \text{c.c.}$, and the intensity wave, $\frac{1}{2} m I_0 \exp(iKx - i\Omega t) + \text{c.c.}$, are present in the medium. Moreover, let us assume that the following spatial and temporal synchronism conditions are fulfilled:

$$\vec{K} + \vec{k}_\beta = \vec{k}_\alpha, \quad \Omega + \omega_\beta = \omega_\alpha. \tag{8}$$

If we insert the *Ansätze* into the parametrically nonlinear term [PN] in Eq. (7) and assume that only the three waves are present in the medium, the terms proportional to $\exp(i\vec{k}_\alpha \cdot \vec{r} - i\omega_\alpha t)$ are given by

$$[\text{PN}]_{\exp(i\vec{k}_\alpha \cdot \vec{r} - i\omega_\alpha t)} = i\bar{U}_{\vec{k}_\alpha; \vec{k}_\beta} \tilde{e}_{\vec{k}_\beta}, \tag{9}$$

where

$$\bar{U}_{\vec{k}_\alpha; \vec{k}_\beta} = -\frac{m}{2} (\bar{\omega}_{\vec{k}_\alpha} - i\gamma_{\vec{k}_\alpha}) \hat{k}_\alpha \cdot \hat{k}_\beta, \tag{10}$$

and $\hat{k}_\alpha, \hat{k}_\beta$ are unit vectors along $\vec{k}_\alpha, \vec{k}_\beta$, respectively. $\bar{U}_{\vec{k}_\alpha; \vec{k}_\beta}$ may be called the coupling coefficient between the $e_{\vec{k}_\alpha}$ wave and the $e_{\vec{k}_\beta}$ wave due to the linking intensity wave.

As a second example, suppose that the two SCFWs from above and a third wave, $e_{\vec{k}_\delta} \exp(i\vec{k}_\delta \cdot \vec{r} - i\omega_\delta t) + \text{c.c.}$, are now the only ones present, where now $\vec{k}_\delta + \vec{k}_\beta = \vec{k}_\alpha$ and $\omega_\delta + \omega_\beta = \omega_\alpha$. Inserting these *Ansätze* in the eigennonlinearity term [EN] in Eq. (7) one can find that the terms proportional to $\exp(i\vec{k}_\alpha \cdot \vec{r} - i\omega_\alpha t)$ are given by

$$[\text{EN}]_{\exp(i\vec{k}_\alpha \cdot \vec{r} - i\omega_\alpha t)} = i\bar{V}_{\vec{k}_\alpha; \vec{k}_\beta, \vec{k}_\delta}(\omega_\beta, \omega_\delta) e_{\vec{k}_\beta} e_{\vec{k}_\delta}, \tag{11}$$

where

$$\begin{aligned}
\bar{V}_{\vec{k}_\alpha; \vec{k}_\beta, \vec{k}_\delta}(\omega_\beta, \omega_\delta) &= \frac{\gamma_{\vec{k}_\alpha} + i\bar{\omega}_{\vec{k}_\alpha}}{i\omega_{\vec{k}_\alpha}} d \left(\hat{k}_\alpha \cdot \hat{k}_\delta \frac{k_\beta}{k_{\alpha,x}} \omega_\beta \right. \\
&\quad \left. + \hat{k}_\alpha \cdot \hat{k}_\beta \frac{k_\delta}{k_{\alpha,x}} \omega_\delta \right). \tag{12}
\end{aligned}$$

The factor $d = (1 + \delta_{\beta\delta})^{-1}$ is a degeneracy factor which equals unity except for the degenerate case where $\beta = \delta$; in this case $d = \frac{1}{2}$. In deriving Eq. (11) we have assumed that the wave amplitudes vary slowly as compared to their oscillation periods $2\pi/\omega_i$. Due to this, we can neglect the $\dot{e}_{\vec{k}_i}$ terms in [EN] (slowly varying amplitude approximation). $\bar{V}_{\vec{k}_\alpha; \vec{k}_\beta, \vec{k}_\delta}(\omega_\beta, \omega_\delta)$ may be referred to as the coupling coefficient between the three SCFWs.

If $k_{\alpha,x}$ is well outside the hatched region in Fig. 3 we have $Q_{\vec{k}_\alpha} \gg 1$ and the expressions for \bar{U} and \bar{V} can be simplified:

$$\bar{U}_{\vec{k}_\alpha; \vec{k}_\beta} \approx U_{\vec{k}_\alpha; \vec{k}_\beta} \equiv -\frac{m}{2} \omega_{\vec{k}_\alpha} \hat{k}_\alpha \cdot \hat{k}_\beta, \tag{13}$$

$$\begin{aligned}
\bar{V}_{\vec{k}_\alpha; \vec{k}_\beta, \vec{k}_\delta}(\omega_\beta, \omega_\delta) &\approx V_{\vec{k}_\alpha; \vec{k}_\beta, \vec{k}_\delta}(\omega_\beta, \omega_\delta) \\
&\equiv d \left(\hat{k}_\alpha \cdot \hat{k}_\delta \frac{k_\beta}{k_{\alpha,x}} \omega_\beta + \hat{k}_\alpha \cdot \hat{k}_\beta \frac{k_\delta}{k_{\alpha,x}} \omega_\delta \right).
\end{aligned}$$

Note that in this case, the U and V coefficients become real. As we shall see, the introduction of the U and V coefficients considerably facilitates the derivation of the coupled amplitude equations in our nonlinear theory. In particular, when many waves are present they appear to be very useful.

III. EXCITATION OF PARAMETRIC WAVES

It is known [28,29] that the nonlinear terms in the wave equation (7) can generate higher order waves with wave vectors $2\vec{K}, 3\vec{K}$, etc. However, at $\varepsilon \approx \frac{1}{4}$, which is the main region of concern in the present paper, these waves are far from resonance and, consequently, their amplitudes are negligibly small. In this section we introduce another type of waves which is also due to the nonlinear terms in the wave equation. These are the parametric waves. The parametric waves always appear in pairs interacting with a third wave, the pump wave, from which they receive their energy. To be

able to do so, they need to meet the following conditions of parametric resonance:

$$\begin{aligned}\vec{k}_S + \vec{k}_I &= \vec{K}, \\ \omega_{\vec{k}_S} + \omega_{\vec{k}_I} &= \Omega,\end{aligned}\quad (14)$$

where $\vec{k}_{S,I}$ are the wave vectors of the parametric waves, $\omega_{\vec{k}_S, \vec{k}_I}$ are the corresponding eigenfrequencies, and \vec{K}, Ω are the wave vectors and frequency of the pump wave. If these conditions are fulfilled the two parametric waves might be excited provided the pump is sufficiently strong.

In the general situation, however, we need to be able to describe also the case where Eqs. (14) are not completely fulfilled. Therefore we allow the parametric waves to assume arbitrary frequencies $\omega_{S,I}$ though still close to their respective eigenfrequencies, i.e., $\omega_{S,I} \cong \omega_{\vec{k}_S, \vec{k}_I}$, and still so that $\omega_S + \omega_I = \Omega$. In this manner the parametric waves may still be considered as having the fundamental properties of eigenwaves.

Let us consider the excitation of parametric waves in our concrete case. Let the fundamental wave with wave vector \vec{K} and frequency Ω act as the pump wave. Apart from this wave there is also some noise in the space-charge field that can be considered as a statistical mixture of many weak waves. If two of these noise waves have wave vectors \vec{k}_S, \vec{k}_I and frequencies ω_S, ω_I meeting the conditions $\vec{k}_S + \vec{k}_I = \vec{K}$ and $\omega_S + \omega_I = \Omega$, they can interact with the fundamental wave via the nonlinear terms in Eq. (7) and start growing in time. We then say that the parametric waves are excited and we have the state of photorefractive parametric oscillation. The parametric waves are sometimes called signal and idler waves which are names taken from similar parametric processes for optical waves [4]. This is why we use the subscripts ‘‘S’’ and ‘‘I’’ for the parametrically conjugated waves. It should be underlined that there is no conceptual difference between these two waves.

Imagine now that at $t=0$ we have the fundamental wave with the amplitude $e_{\vec{K}}$ and two parametric waves with amplitudes $e_{\vec{k}_S}$ and $e_{\vec{k}_I}$ on noise level, i.e., they are very small. For a sufficiently small period of time while the parametric amplitudes are still relatively small, we can assume that the fundamental wave is not affected by the parametric waves. Hence, at this stage the nonlinear terms in Eq. (7) are negligible in the equation for $\vec{k}_\alpha = \vec{K}$ and, as a result, $e_{\vec{K}}$ may be set equal to $e_{\vec{K},L}$. As regards the parametric waves with the wave vectors $\vec{k}_\alpha = \vec{k}_{S,I}$, the nonlinear sum in Eq. (7) includes terms proportional to the large amplitude $e_{\vec{K},L}$. Hence, nonlinear effects are important for these two waves. The corresponding amplitude equations may be derived assuming the following form of the space-charge field:

$$\begin{aligned}\vec{E}_1 &= E_0 [\hat{x} e_{\vec{K},L} \exp(iKx - i\Omega t) + \hat{k}_S e_{\vec{k}_S} \exp(i\vec{k}_S \cdot \vec{r} - i\omega_S t) \\ &\quad + \hat{k}_I e_{\vec{k}_I} \exp(i\vec{k}_I \cdot \vec{r} - i\omega_I t) + \text{c.c.}],\end{aligned}\quad (15)$$

where $e_{\vec{k}_S}(t)$ and $e_{\vec{k}_I}(t)$ are the amplitudes of the parametric waves. By inserting Eq. (15) in Eq. (7) and using Eqs. (9) and (11) we arrive at the following amplitude equations:

$$\begin{aligned}\dot{e}_{\vec{k}_S} + [\gamma_{\vec{k}_S} + i(\bar{\omega}_{\vec{k}_S} - \omega_S)] e_{\vec{k}_S} \\ = -i\bar{U}_{\vec{k}_S; -\vec{k}_I} e_{\vec{k}_I}^* - i\bar{V}_{\vec{k}_S; -\vec{k}_I, \vec{K}}(-\omega_I, \Omega) e_{\vec{K},L} e_{\vec{k}_I}^*,\end{aligned}\quad (16)$$

$$\begin{aligned}\dot{e}_{\vec{k}_I} + [\gamma_{\vec{k}_I} + i(\bar{\omega}_{\vec{k}_I} - \omega_I)] e_{\vec{k}_I} \\ = -i\bar{U}_{\vec{k}_I; -\vec{k}_S} e_{\vec{k}_S}^* - i\bar{V}_{\vec{k}_I; -\vec{k}_S, \vec{K}}(-\omega_S, \Omega) e_{\vec{K},L} e_{\vec{k}_S}^*,\end{aligned}\quad (17)$$

In deriving Eqs. (16) and (17) we have assumed that $e_{\vec{k}_S}$ and $e_{\vec{k}_I}$ are slowly varying, i.e., $\dot{e}_{\vec{k}_S} \ll \omega_S e_{\vec{k}_S}$ and $\dot{e}_{\vec{k}_I} \ll \omega_I e_{\vec{k}_I}$. The set of equations (16), (17) has a solution of the form $e_{\vec{k}_S} \propto \exp(\nu t)$ and $e_{\vec{k}_I} \propto \exp(\nu t)$, where ν is referred to as the increment. Using this representation we obtain

$$[\nu + \gamma + i(\omega_{\vec{k}_S} - \omega_S)] e_{\vec{k}_S} = -ih_S e_{\vec{k}_I}^*,\quad (18)$$

$$[\nu + \gamma - i(\omega_{\vec{k}_I} - \omega_I)] e_{\vec{k}_I} = ih_I e_{\vec{k}_S}^*,\quad (19)$$

where the coupling coefficients h_S and h_I are given by

$$\begin{aligned}h_S &= U_{\vec{k}_S; -\vec{k}_I} + V_{\vec{k}_S; -\vec{k}_I, \vec{K}}(-\omega_S, \Omega) e_{\vec{K},L}, \\ h_I &= U_{\vec{k}_I; -\vec{k}_S} + V_{\vec{k}_I; -\vec{k}_S, \vec{K}}(-\omega_I, \Omega) e_{\vec{K},L},\end{aligned}\quad (20)$$

In Eqs. (18),(19) we have assumed that $\gamma_{\vec{k}_S} \cong \gamma_{\vec{k}_I} \cong \gamma$, which holds true if the longitudinal components of \vec{k}_S and \vec{k}_I are not far from $\vec{K}/2$. Furthermore, in Eqs. (20) we have assumed that \vec{k}_S, \vec{k}_I are outside the hatched region in Fig. 3, so that $\bar{U}_{\vec{k}_S; -\vec{k}_I} \cong U_{\vec{k}_S; -\vec{k}_I}$ and $\bar{V}_{\vec{k}_S; -\vec{k}_I, \vec{K}}(-\omega_S, \Omega) \cong V_{\vec{k}_S; -\vec{k}_I, \vec{K}}(-\omega_S, \Omega)$. As a consequence, the coupling coefficients become real parameters. The linear system of algebraic equations (18),(19) involves the unknowns ν and ω_S (since $\omega_I = \Omega - \omega_S$).

To obtain a nontrivial solution for $e_{\vec{k}_S}, e_{\vec{k}_I}^*$ we should equalize to zero the determinant of this system which gives us the characteristic equation. From the imaginary part of this equation together with the temporal synchronism condition we obtain

$$\omega_S = \omega_{\vec{k}_S} + \Delta, \quad \omega_I = \omega_{\vec{k}_I} + \Delta,\quad (21)$$

$$\Delta = \frac{1}{2} [\Omega - (\omega_{\vec{k}_S} + \omega_{\vec{k}_I})].$$

As is seen, Δ represents the parametric waves' detuning from their eigenfrequencies.

From the real part of the characteristic equation we obtain

$$\nu_{\pm} = -\gamma \pm \sqrt{h_S h_I - \Delta^2}.\quad (22)$$

If the increment ν_+ is positive (ν_- is always negative) the parametric wave amplitudes increase exponentially in time and we can say that the fundamental wave is unstable against excitation of the parametric waves.

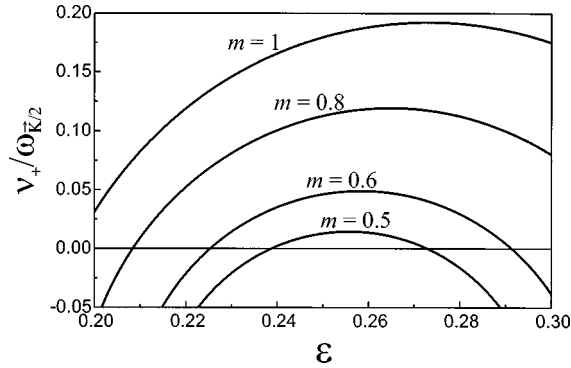


FIG. 4. Normalized increment $v_+/\omega_{\vec{k}/2}$ versus ε for different values of m .

To obtain the explicit dependence on the parametric wave vectors \vec{k}_S and \vec{k}_I we introduce the following representation:

$$\vec{k}_S = \frac{K}{2} [(1+X)\hat{x} + Y\hat{y}], \quad \vec{k}_I = \frac{K}{2} [(1-X)\hat{x} - Y\hat{y}], \quad (23)$$

where \hat{x} and \hat{y} are unit vectors along the longitudinal and transversal directions. The dimensionless parameters X and Y thus express, respectively, the longitudinal and transversal split between the parametric wave vectors. In the simplest case of degenerate parametric oscillation ($\vec{K}/2$ subharmonic case), we have $X=Y=0$. In the case of transversal parametric oscillation we have $X=0$ and $Y \neq 0$. In this case ν_+ can be written in the following simple form provided that $|1-4\varepsilon|, Y \ll 1$:

$$\frac{\nu_+}{\omega_{\vec{k}/2}} \cong -Q_{\vec{k}/2}^{-1} + \left(\frac{m^2}{9} \left[1 - 2Y^2 - \frac{5}{3}(1-4\varepsilon) \right] - (1-4\varepsilon)^2 \right)^{1/2}, \quad (24)$$

where the first term under the radical originates from the product $h_S h_I$, the last term from Δ^2 . Equation (24) represents a simplified version of a similar expression obtained in Ref. [11]. One can see from Eq. (24) that a large quality factor $Q_{\vec{k}/2}$ and a large intensity contrast m both favor the instability whereas increasing Y suppresses the instability. It means, in particular, that the degenerate case ($Y=0$) is characterized by the largest increment. As regards the dependence on ε this is displayed for different values of m in Fig. 4 for the case $Y=0$ and $Q_{\vec{k}/2}=6.5$ (typical for sillenites, see Fig. 3). First of all, it is seen that the maximum normalized increment does not exceed 0.2. This means that the slowly varying amplitude approximation holds true in all the cases considered. Secondly, one sees that the maximum increment is obtained for $0.25 \leq \varepsilon \leq 0.28$. From Eq. (22) one might think that $\Delta=0$ (i.e., $\varepsilon=0.25$) would give maximum increment. The reason why the optimum values of ε are slightly shifted upwards is that $h_S h_I$ increases with ε , as seen in Eq. (24), due to which the optimum value of ε is slightly shifted upwards by $m^2/43$. Thus for some small region beyond $\varepsilon = \frac{1}{4}$ the detuning from resonance of the parametric waves is compensated by the increase of the coupling coefficients.

One has to bear in mind, however, that higher order corrections to the linear theory might be significant, especially for m close to unity, so that the maximums in Fig. 4 might be slightly altered [23].

By setting $\nu_+=0$ in Eq. (24) one can find the threshold condition for the instability. The threshold value for the contrast can thus be found to give

$$m_{\text{th}} = 3 \left(\frac{Q_{\vec{k}/2}^{-2} + (1-4\varepsilon)^2}{1-2Y^2 - \frac{5}{3}(1-4\varepsilon)} \right)^{1/2}. \quad (25)$$

A useful parameter to be used in the next sections is the supercriticality ξ defined by

$$\xi = \sqrt{h_S h_I - \gamma^2}. \quad (26)$$

From Eq. (22) one can see that if $|\Delta| < \xi$ the increment is positive and the parametric waves grow exponentially.

IV. FORCED WAVES AND NONLINEAR FREQUENCY SHIFTS

In Sec. III we considered the situation where only the strong fundamental wave and the two weak parametric waves were present in the medium. We saw that the fundamental wave can become unstable against exponential growth of the parametric waves. Naturally, after some time of exponential growth we can no longer consider the parametric waves as weak, so to be able to describe the stabilization (saturation) of the growth we need to modify the linear theory. What happens as the parametric waves become stronger? They start to generate so-called forced waves. These waves are generated when two strong waves interact via the nonlinear terms in Eq. (7) and produce forced sum or difference waves with temporal and spatial frequencies that equal the sum or difference between the two strong waves' frequencies. Moreover, to be considered as forced, a wave should be driven far from resonance. It means that if a forced wave is driven at the wave vector \vec{k} and frequency ω , then ω should be far from $\omega_{\vec{k}}$.

What is the effect of forced waves apart from just being present in the medium? Can they disturb the original fundamental and parametric waves? Indeed they can; they can take part in further three-wave interactions with the original waves and thereby alter their amplitudes. In the present paper all forced waves are generated with participation of at least one parametric wave. Therefore, as a general example, let us consider the effect of the forced wave formed by the summation of the parametric S wave and another arbitrary wave with wave vector \vec{k}_α and frequency ω_α . To find the amplitude of this forced wave which has the wave vector $\vec{k}_S + \vec{k}_\alpha$ and frequency $\omega_S + \omega_\alpha$ we use the following solution *Ansatz* in Eq. (7):

$$\begin{aligned} \vec{E}_1 = E_0 \{ & \hat{k}_S e_{\vec{k}_S} \exp(i\vec{k}_S \cdot \vec{r} - i\omega_S t) + \hat{k}_\alpha e_{\vec{k}_\alpha} \exp(i\vec{k}_\alpha \cdot \vec{r} - i\omega_\alpha t) \\ & + \hat{u}_{\vec{k}_S + \vec{k}_\alpha} e_{\vec{k}_S + \vec{k}_\alpha} \exp[i(\vec{k}_S + \vec{k}_\alpha) \cdot \vec{r} - i(\omega_S + \omega_\alpha)t] + \text{c.c.} \}, \end{aligned} \quad (27)$$

and neglect for a moment all other waves. Here $\hat{u}_{\vec{k}_S + \vec{k}_\alpha}$ de-

notes a unit vector along $\vec{k}_S + \vec{k}_\alpha$ and $e_{\vec{k}_S + \vec{k}_\alpha}$ is the amplitude of the forced wave. By singling out the terms proportional to $\exp[i(\vec{k}_S + \vec{k}_\alpha) \cdot \vec{r} - i(\omega_S + \omega_\alpha)t]$ one can obtain the following amplitude equation:

$$\begin{aligned} & \left[\frac{d}{dt} + \gamma_{\vec{k}_S + \vec{k}_\alpha} + i[\omega_{\vec{k}_S + \vec{k}_\alpha} - (\omega_S + \omega_\alpha)] \right] e_{\vec{k}_S + \vec{k}_\alpha} \\ & = i\delta_{\alpha F} U_{\vec{k}_S + \vec{k}_\alpha; \vec{k}_S} e_{\vec{k}_S} + iV_{\vec{k}_S + \vec{k}_\alpha; \vec{k}_S, \vec{k}_\alpha}(\omega_S, \omega_\alpha) e_{\vec{k}_\alpha} e_{\vec{k}_S}, \end{aligned} \quad (28)$$

where the Kronecker delta $\delta_{\alpha F}$ accounts for the case where $\vec{k}_\alpha = \vec{k}_F \equiv \vec{K}$; in this case the intensity wave also takes part in the generation of the forced wave.

We now introduce an important simplification. By using the fact that the forced wave is excited far from resonance and that $Q_{\vec{k}_S + \vec{k}_\alpha} \gg 1$, we can neglect the terms d/dt

+ $\gamma_{\vec{k}_S + \vec{k}_\alpha}$ in comparison with the large term $i[\omega_{\vec{k}_S + \vec{k}_\alpha} - (\omega_S + \omega_\alpha)]$ on the left-hand side of Eq. (28), which expresses the detuning from resonance. As a consequence of this, the forced amplitude $e_{\vec{k}_S + \vec{k}_\alpha}$ is immediately obtained:

$$\begin{aligned} e_{\vec{k}_S + \vec{k}_\alpha} & = \delta_{\alpha F} \frac{U_{\vec{k}_S + \vec{k}_\alpha; \vec{k}_S}}{\omega_{\vec{k}_S + \vec{k}_\alpha} - (\omega_S + \omega_\alpha)} e_{\vec{k}_S} \\ & + \frac{V_{\vec{k}_S + \vec{k}_\alpha; \vec{k}_S, \vec{k}_\alpha}(\omega_S, \omega_\alpha)}{\omega_{\vec{k}_S + \vec{k}_\alpha} - (\omega_S + \omega_\alpha)} e_{\vec{k}_\alpha} e_{\vec{k}_S}. \end{aligned} \quad (29)$$

We are now ready to determine the influence of this forced wave on the parametric S wave with amplitude $e_{\vec{k}_S}$. By singling out the terms in Eq. (7) that are proportional to $\exp(i\vec{k}_S \cdot \vec{r} - i\omega_S t)$ one can find

$$\begin{aligned} & \left[\frac{d}{dt} + \gamma_{\vec{k}_S} + i(\omega_{\vec{k}_S} - \omega_S) \right] e_{\vec{k}_S} = -iU_{\vec{k}_S; -\vec{k}_I} e_{\vec{k}_I}^* - iV_{\vec{k}_S; \vec{K}, -\vec{k}_I}(\Omega, -\omega_I) e_{\vec{K}, L} e_{\vec{k}_I}^* + i\delta_{\alpha F} U_{\vec{k}_S; \vec{k}_S + \vec{k}_\alpha} e_{\vec{k}_S + \vec{k}_\alpha} \\ & - iV_{\vec{k}_S; \vec{k}_S + \vec{k}_\alpha, -\vec{k}_\alpha}(\omega_S + \omega_\alpha, -\omega_\alpha) e_{\vec{k}_S + \vec{k}_\alpha} e_{\vec{k}_\alpha}^*, \end{aligned} \quad (30)$$

where we assume that $\vec{k}_S + \vec{k}_\alpha$ is well outside the hatched region in Fig. 3. If one compares Eq. (30) with Eq. (16) it is seen that the last two terms on the right-hand side of Eq. (30) represent the correction due to the forced $e_{\vec{k}_S + \vec{k}_\alpha}$ wave. If, in Eq. (30), one substitutes $e_{\vec{k}_S + \vec{k}_\alpha}$ with the expression from Eq. (29) one can obtain

$$\dot{e}_{\vec{k}_S} + [\gamma_{\vec{k}_S} + i(\omega_{\vec{k}_S}^{\text{nl}} - \omega_S)] e_{\vec{k}_S} = -ih_S e_{\vec{k}_I}^*, \quad (31)$$

where h_S is given by Eq. (20). The influence of the $e_{\vec{k}_S + \vec{k}_\alpha}$ wave is thus represented in a modified eigenfrequency $\omega_{\vec{k}_S}^{\text{nl}}$, called the nonlinear eigenfrequency, which equals the linear eigenfrequency $\omega_{\vec{k}_S}$, plus a correction $\delta\omega_{\vec{k}_S, \vec{k}_S + \vec{k}_\alpha}$, called the nonlinear frequency shift,

$$\begin{aligned} \delta\omega_{\vec{k}_S, \vec{k}_S + \vec{k}_\alpha} & = -\delta_{\alpha F} \left(\frac{U_{\vec{k}_S; \vec{k}_S + \vec{K}} U_{\vec{k}_S + \vec{K}; \vec{k}_S}}{\omega_{\vec{k}_S + \vec{K}} - (\omega_S + \Omega)} + \frac{U_{\vec{k}_S; \vec{k}_S + \vec{K}} V_{\vec{k}_S + \vec{K}; \vec{k}_S, \vec{K}}(\omega_S, \Omega)}{\omega_{\vec{k}_S + \vec{K}} - (\omega_S + \Omega)} e_{\vec{K}, L} \right. \\ & \left. - \frac{V_{\vec{k}_S; \vec{k}_S + \vec{K}, -\vec{K}}(\omega_S - \Omega, -\Omega) U_{\vec{k}_S + \vec{K}; \vec{k}_S}}{\omega_{\vec{k}_S + \vec{K}} - (\omega_S + \Omega)} e_{\vec{K}, L} \right) + T_{\vec{k}_S, \vec{k}_S + \vec{k}_\alpha} N_{\vec{k}_\alpha}, \end{aligned} \quad (32)$$

where

$$T_{\vec{k}_S, \vec{k}_S + \vec{k}_\alpha} = z_{\vec{k}_\alpha + \vec{k}_S} \frac{V_{\vec{k}_S; \vec{k}_S + \vec{k}_\alpha, -\vec{k}_\alpha}(\omega_S + \omega_\alpha, -\omega_\alpha) V_{\vec{k}_S + \vec{k}_\alpha; \vec{k}_S, \vec{k}_\alpha}(\omega_S, \omega_\alpha)}{\omega_{\vec{k}_S + \vec{k}_\alpha} - (\omega_S + \omega_\alpha)}, \quad (33)$$

and $N_{\vec{k}_\alpha} = |e_{\vec{k}_\alpha}|^2$. The factor $z_{\vec{k}_\alpha + \vec{k}_S}$ in Eq. (33) equals zero if $\vec{k}_\alpha + \vec{k}_S = 0$ and unity otherwise. It is included to take into account that any forced wave with wave vector $\vec{0}$ vanishes and thus cannot give rise to any frequency shift. This is because the spatially averaged electric field is fixed and equals \vec{E}_0 . In a similar manner as for the $e_{\vec{k}_S + \vec{k}_\alpha}$ wave, all other forced waves can be represented by their frequency

shifts of the parametric eigenfrequencies, so that in total one ends up with the two modified amplitude equations for the parametric waves:

$$\dot{e}_{\vec{k}_S} + [\gamma_{\vec{k}_S} + i(\omega_{\vec{k}_S}^{\text{nl}} - \omega_S)] e_{\vec{k}_S} = -ih_S e_{\vec{k}_I}^*, \quad (34)$$

$$\dot{e}_{\vec{k}_I}^* + [\gamma_{\vec{k}_I} - i(\omega_{\vec{k}_I}^{\text{nl}} - \omega_I)] e_{\vec{k}_I}^* = ih_I e_{\vec{k}_S}, \quad (35)$$

where the influences of all the forced waves are included in $\omega_{k_S}^{\text{nl}}$ and $\omega_{k_I}^{\text{nl}}$. As for Eqs. (18), (19) the solutions to Eqs. (34) and (35) assume the form $e_{k_S}^{\sim}, e_{k_I}^{\ast} \propto \exp(\nu t)$ by which one can obtain

$$\begin{aligned} \omega_S &= \omega_{k_S}^{\text{nl}} + \Delta_{\text{nl}}, & \omega_I &= \omega_{k_I}^{\text{nl}} + \Delta_{\text{nl}}, \\ \nu_+ &= -\gamma + \sqrt{h_S h_I - \Delta_{\text{nl}}^2}, & (36) \\ \Delta_{\text{nl}} &= \frac{1}{2}[\Omega - (\omega_{k_S}^{\text{nl}} + \omega_{k_I}^{\text{nl}})]. \end{aligned}$$

There is, however, a technical problem with Eqs. (36). ω_S and ω_I are not easily determined from these equations because $\omega_{k_S}^{\text{nl}}$ and $\omega_{k_I}^{\text{nl}}$ depend explicitly on ω_S and ω_I in a rather complicated manner, as can be seen from Eq. (32). A way to get around this problem is to use the fact that the parametric waves are nearly eigenwaves, i.e., $\omega_S \approx \omega_{k_S}^{\sim}, \omega_I \approx \omega_{k_I}^{\sim}$, and then simply replace ω_S by $\omega_{k_S}^{\sim}$ and ω_I by $\omega_{k_I}^{\sim}$ in the expression for $\omega_{k_S}^{\text{nl}}$ and $\omega_{k_I}^{\text{nl}}$. In the case of transversal parametric oscillation, however, we know that $\omega_S = \omega_I = \Omega/2$ in which case no problem appears.

As demonstrated above, one can significantly simplify the calculations of including forced waves by using the concept of nonlinear frequency shift, a concept that was introduced in the field of PPO recently [22]. The alternative would be to solve $N+2$ nonlinear differential equations, where N is the number of forced waves. With the present technique the problem is reduced to that of solving two linear differential equations given by Eqs. (34) and (35).

V. STEADY STATE FOR THE PARAMETRIC WAVES

In this section we use the technique of representing forced waves by their nonlinear frequency shifts to describe the stationary states of the parametric waves.

As the parametric waves grow they start to interact with themselves and the fundamental wave via the generation of forced waves. Hence, in principle, all possible sum and difference waves formed by the two parametric waves and the fundamental wave should be taken into account, i.e., waves with wave vectors $\vec{k}_S \pm \vec{k}_S, \vec{k}_S \pm \vec{k}_I, \vec{k}_S \pm \vec{K}, \vec{k}_I \pm \vec{k}_I$, and $\vec{k}_I \pm \vec{K}$. However, a few of these waves need to be removed from the list: (i) the $\vec{k}_S - \vec{k}_S$ and $\vec{k}_I - \vec{k}_I$ waves vanish because they have wave vectors equal to $\vec{0}$, (ii) the waves with wave vectors $\vec{k}_{S,I} - \vec{K}$ are identical to the parametric waves and thus cannot be considered as forced. As a consequence, the number of forced waves to be included reduces to six. As demonstrated in Sec. IV, the influence of the forced waves can be represented by nonlinear modifications to the eigenfrequencies of the S and I waves, so taking the remaining six waves into account we obtain

$$\begin{aligned} \omega_{k_S}^{\text{nl}} &= \omega_{k_S}^{\sim} + \delta\omega_{k_S, \vec{k}_S + \vec{k}_S}^{\sim} + \delta\omega_{k_S, \vec{k}_S + \vec{K}}^{\sim} + \delta\omega_{k_S, \vec{k}_S + \vec{k}_I}^{\sim} \\ &+ \delta\omega_{k_S, \vec{k}_S - \vec{k}_I}^{\sim}, \end{aligned} \quad (37)$$

$$\omega_{k_I}^{\text{nl}} = \omega_{k_I}^{\sim} + \delta\omega_{k_I, \vec{k}_I + \vec{k}_I}^{\sim} + \delta\omega_{k_I, \vec{k}_I + \vec{K}}^{\sim} + \delta\omega_{k_I, \vec{k}_I + \vec{k}_S}^{\sim} + \delta\omega_{k_I, \vec{k}_I - \vec{k}_S}^{\sim},$$

It is worthy of note that the forced $\vec{k}_S + \vec{k}_I$ wave is considered isolated from the fundamental wave even though they have identical wave vectors and frequencies. One could add the two waves and then obtain a renormalized fundamental wave. In this presentation, however, we prefer to think of the two waves as separate due to which the $\vec{k}_S + \vec{k}_I$ wave is acting as a nonlinear frequency shift, as seen in Eq. (37). Hence, the index \vec{K} always refers to the linear fundamental wave with amplitude $e_{\vec{K},L}$. Whatever representation is used, though, the same result is obtained.

At first sight, one might think that there is a problem with the shifts $\delta\omega_{k_S, \vec{k}_S - \vec{k}_I}^{\sim}$ and $\delta\omega_{k_I, \vec{k}_I - \vec{k}_S}^{\sim}$ in Eq. (37) because Eq. (32) was derived under the assumption that \vec{k}_S and $\vec{k}_S + \vec{k}_I$ have sufficiently large x components. But the vector $\vec{k}_S - \vec{k}_I$ may have a very small x component when $k_{I,x}$ approaches $k_{S,x}$. Therefore we have to consider the validity of Eq. (32) in this case. The key question to be asked is whether the expression for the forced wave amplitude $e_{\vec{k}_S - \vec{k}_I}^{\sim}$ can be simplified in the following way:

$$\begin{aligned} e_{\vec{k}_S - \vec{k}_I}^{\sim} &= i \frac{\bar{V}_{\vec{k}_S - \vec{k}_I; \vec{k}_S, -\vec{k}_I}(\omega_S, -\omega_I)}{\gamma_{\vec{k}_S - \vec{k}_I} + i(\bar{\omega}_{\vec{k}_S - \vec{k}_I} - \omega_S + \omega_I)} e_{-\vec{k}_I}^{\sim} e_{\vec{k}_S}^{\sim} \\ &\equiv \frac{V_{\vec{k}_S - \vec{k}_I; \vec{k}_S, -\vec{k}_I}(\omega_{k_S}^{\sim}, -\omega_{k_I}^{\sim})}{\omega_{\vec{k}_S - \vec{k}_I}^{\sim} - \omega_{k_S}^{\sim} + \omega_{k_I}^{\sim}} e_{-\vec{k}_I}^{\sim} e_{\vec{k}_S}^{\sim}, \end{aligned} \quad (38)$$

when $k_{S,x}$ approaches $k_{I,x}$? If we use Eqs. (12) and (13) in Eq. (38) and cancel common factors one can find that the left- and right-hand sides of Eq. (38) can be represented by

$$\begin{aligned} f_e \exp(i\phi_e) &= -\frac{\gamma_{\vec{k}_S - \vec{k}_I} + i\bar{\omega}_{\vec{k}_S - \vec{k}_I}}{\omega_{\vec{k}_S - \vec{k}_I}^{\sim} [\gamma_{\vec{k}_S - \vec{k}_I} + i(\bar{\omega}_{\vec{k}_S - \vec{k}_I} - \omega_{k_S}^{\sim} + \omega_{k_I}^{\sim})]}, \\ f_s &= -\frac{1}{\omega_{\vec{k}_S - \vec{k}_I}^{\sim} - \omega_{k_S}^{\sim} + \omega_{k_I}^{\sim}}, \end{aligned} \quad (39)$$

respectively. If we use the representations for \vec{k}_S and \vec{k}_I from Eq. (23) and, as an example, set $Y=0$ we can investigate f_e and f_s for small values of X . The two functions are plotted in Fig. 5. As is seen, f_s approaches f_e when X goes to zero ($k_{I,x} \rightarrow k_{S,x}$). Moreover, the phase of f_e is only a few degrees which ensures that the frequency shift remains real. In conclusion, we can use Eq. (32) in all actual cases.

The presence of the forced waves is now included in $\omega_{k_S}^{\text{nl}}$ and $\omega_{k_I}^{\text{nl}}$ from Eq. (37). To find the stationary amplitudes of $e_{k_S}^{\sim}$ and $e_{k_I}^{\sim}$ we can simply use Eqs. (34) and (35) and set the d/dt terms equal to 0 after which we obtain

$$[\gamma - i\Delta_{\text{nl}}]e_{k_S}^{\sim} = -ih_S e_{k_I}^{\ast}, \quad (40)$$

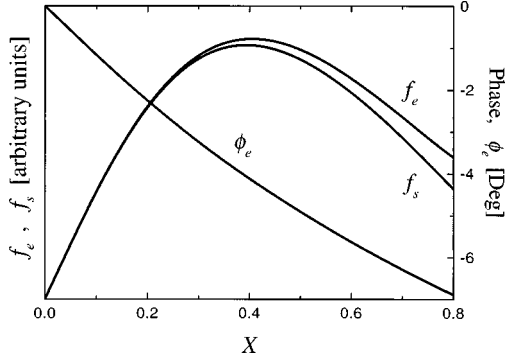


FIG. 5. Plots of the functions f_e and f_s and of the phase ϕ_e versus X . Again, the same parameters as in Fig. 3 have been used along with $K = 2\pi/30 \mu\text{m}^{-1}$.

$$[\gamma + i\Delta_{\text{nl}}]e_{k_I}^* = ih_I e_{k_S}^*, \quad (41)$$

where Δ_{nl} is given by Eq. (36) with $\omega_{k_S}^{\text{nl}}$ and $\omega_{k_I}^{\text{nl}}$ taken from Eqs. (37).

From Eqs. (40) and (41) one can immediately find the following important relation for the amplitude product $\sigma = e_{k_S}^* e_{k_I}$:

$$\sigma \equiv |\sigma| \exp(-i\Psi) = \frac{-ih_S N_I}{\gamma - i\Delta_{\text{nl}}} = \frac{-ih_I N_S}{\gamma - i\Delta_{\text{nl}}}. \quad (42)$$

Moreover, from the condition that the determinant of Eqs. (40) and (41) should equal zero one can obtain

$$\gamma^2 + \Delta_{\text{nl}}^2 = h_S h_I \Leftrightarrow \Delta_{\text{nl}}^2 = \xi^2, \quad (43)$$

where the sign \Leftrightarrow is used between equivalent equations. By combining Eqs. (40), (41), and (43) we obtain further

$$N_{k_S}^* = \left(\frac{h_S}{h_I}\right)^{1/2} |\sigma|,$$

$$N_{k_I}^* = \left(\frac{h_I}{h_S}\right)^{1/2} |\sigma|,$$

$$\exp(-i\Psi_{\pm}) = \text{sgn}[h_S] \frac{-i\gamma \mp \xi}{\sqrt{h_S h_I}}. \quad (44)$$

Finally, by using Eqs. (32),(37) together with Eqs. (43) and (44) we get

$$\Delta_{\text{nl}} = \Delta - D - T|\sigma| \Leftrightarrow |\sigma| = \frac{\Delta - D - \Delta_{\text{nl}}}{T}, \quad (45)$$

where

$$D = \frac{1}{2}(\delta\omega_{k_S, \vec{k}_S + \vec{K}} + \delta\omega_{k_I, \vec{k}_I + \vec{K}}),$$

$$T = \frac{T_{k_S, \vec{k}_S + \vec{K}} + T_{k_I, \vec{k}_I + \vec{K}} + T_{k_I, \vec{k}_I - \vec{K}}}{2} \left(\frac{h_S}{h_I}\right)^{1/2} + \frac{T_{k_I, \vec{k}_I + \vec{K}} + T_{k_S, \vec{k}_S + \vec{K}} + T_{k_S, \vec{k}_S - \vec{K}}}{2} \left(\frac{h_I}{h_S}\right)^{1/2}. \quad (46)$$

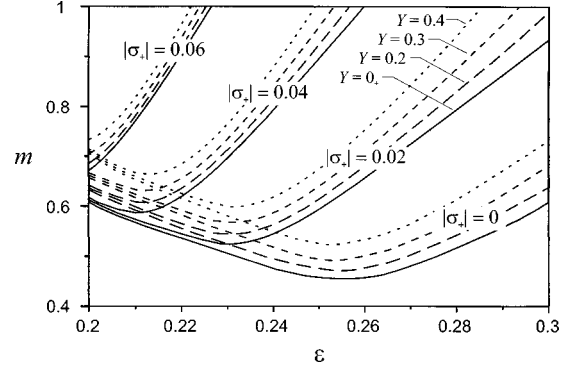


FIG. 6. $|\sigma_+|$ versus ϵ and m for different values of Y . The solid, long dashed, medium dashed, and short dashed lines represent the cases $Y = 0_+, 0.2, 0.3$, and 0.4 , respectively.

From Eq. (43) we see that Δ_{nl} can assume two values, $\pm \xi$, due to which we obtain the two stationary solutions

$$|\sigma_{\pm}| = \frac{\Delta - D \pm \xi}{T}. \quad (47)$$

Note that apart from the two σ_{\pm} solutions we also have the trivial solution, $\sigma_0 = 0$. Expressed by Eqs. (44) and (47), we have now derived the stationary amplitudes of the parametric waves. The parameter D corresponds to the nonlinear frequency shifts due to the $\vec{k}_{S,I} + \vec{K}$ waves whereas T corresponds to the shifts from the $\vec{k}_S \pm \vec{k}_I$, $\vec{k}_S + \vec{k}_S$, and $\vec{k}_I + \vec{k}_I$ waves.

Let us consider the expressions for $|\sigma_+|$ in the case of transversal parametric oscillation, i.e., $X = 0$ and $Y \neq 0$. In this case we have $N_{k_S}^* = N_{k_I}^* = |\sigma|$, thus $|\sigma|$ represents here the modulus square of the amplitudes (energy) of the parametric waves. For this particular case, the parameters entering Eq. (47) assume the following simple form:

$$\frac{\Delta}{\omega_{\vec{K}/2}} \cong 1 - 4\epsilon,$$

$$\frac{D}{\omega_{\vec{K}/2}} \cong \frac{\epsilon^2 m^2}{(4\epsilon + 3)(1 - \epsilon)^2} \left[4\epsilon \left(1 - \frac{5}{18} Y^2\right) + \frac{3}{2} \frac{1}{2} Y^2 \right],$$

$$\frac{\xi}{\omega_{\vec{K}/2}} \cong \left(-Q_{\vec{K}/2}^{-2} + \frac{m^2 \epsilon^2}{(1 - \epsilon)^2} (1 - 2Y^2) \right)^{1/2}, \quad (48)$$

$$\frac{T}{\omega_{\vec{K}/2}} \cong 5 - \frac{11}{3} Y^2,$$

where terms of order Y^4 and higher have been neglected. From Eqs. (47) and (48) it is seen that (i) being positive, the nonlinear frequency shift D due to the $\vec{k}_{S,I} + \vec{K}$ waves reduces $|\sigma_+|$, (ii) $|\sigma_+|$ increases with the quality factor $Q_{\vec{K}/2}$, and (iii) the nonlinear shifts represented by T reduce $|\sigma_+|$; in fact, $|\sigma_+|$ would go to infinity in the absence of these waves. Using Eqs. (47) and (48) a contour plot of $|\sigma_+|$ versus ϵ and m can be obtained, see Fig. 6. It is seen that $|\sigma_+|$ increases with m and decreases with Y . As regards the dependence on ϵ , $|\sigma_+|$ has a maximum that moves from $\epsilon \cong 0.25$ towards lower values as m increases. There is a peculiarity when Y

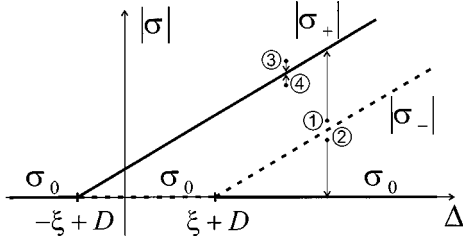


FIG. 7. Schematic diagram of the modulus of the three steady state solutions, σ_0 and σ_{\pm} as functions of Δ . Stable branches are represented by solid lines whereas unstable branches are represented by dashed lines.

goes to zero. In this limit the waves with wave vectors $\vec{k}_S + \vec{k}_S$ and $\vec{k}_I + \vec{k}_I$ become identical to the wave with wave vector $\vec{k}_S + \vec{k}_I$, hence, we have degeneracy. This causes T to jump from 5 at $Y=0_+$ to $\frac{10}{3}$ at $Y=0$; thus $|\sigma_+|$ experiences a corresponding jump upwards in this limit. Therefore an infinitely small transversal split between the parametric wave vectors causes the energy of the parametric waves to be reduced by $\frac{1}{3}$. This was discussed further in Ref. [22].

VI. INTERNAL STABILITY OF THE PARAMETRIC WAVES

In Sec. V we found three steady state solutions σ_0 and σ_{\pm} . The moduli of the three solutions are plotted schematically versus Δ in Fig. 7. The question is now, are these solutions stable? In general, one can distinguish between two types of stability: internal and external. Internal stability means stability of a stationary solution against perturbations in amplitude or phase; external stability means stability against excitation of new waves. In this way, one can say that the fundamental wave is externally unstable, since the instability appears as growth of two additional parametric waves. This section deals with the internal stability analysis of the stationary solutions found in Sec. V.

Let us consider the modulus of the steady state solutions, represented by $|\sigma_i|$ ($i=0, -, +$), and add a small perturbation to it, $\delta|\sigma_i|$, so that the new perturbed steady state is $|\sigma'_i| = |\sigma_i| + \delta|\sigma_i|$. What happens after this perturbation? Will the perturbed state decay back to the original state? To answer this we need to consider Eq. (36) for the increment which depends via Δ_{nl} on the amplitudes of the parametric waves. For the steady state solutions, ν_+ given by Eq. (36) equals zero. If we linearize this equation for the perturbed amplitudes around the stationary amplitudes we obtain the increment

$$\nu_+ = -\gamma + \sqrt{\gamma^2 + 2\Delta_{nl}T\delta|\sigma_i|} \cong \frac{\Delta_{nl}T\delta|\sigma_i|}{\gamma}. \quad (49)$$

If ν_+ is positive, the perturbed amplitudes will increase; if ν_+ is negative they will decrease. Let us analyze the stability of the solutions σ_{\pm} . γ is always positive. T is positive too for the cases considered here, see Eq. (48). As regards Δ_{nl} , this equals the supercriticality ξ for $|\sigma_i| = |\sigma_-|$ and $-\xi$ for $|\sigma_i| = |\sigma_+|$. Let us first consider $|\sigma_i| = |\sigma_-|$. In this case we have $\nu_+ = \xi T \delta|\sigma_-| / \gamma$. From this, it follows that if $\delta|\sigma_-|$ is positive (case ① in Fig. 7) ν_+ is positive too. It means that

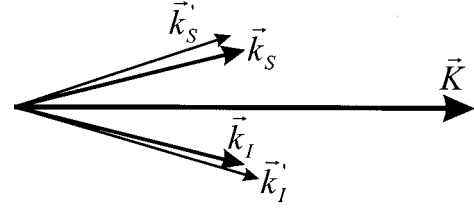


FIG. 8. Wave vector scheme for the primary parametric waves, $\vec{k}_{S,I}$, and the secondary parametric waves, $\vec{k}'_{S,I}$.

the parametric wave amplitudes increase and so does $|\sigma|$. If, on the other hand, $\delta|\sigma_-|$ is negative (case ② in Fig. 7) ν_+ is negative and $|\sigma|$ decreases. Hence, in total, any perturbation, positive or negative, away from σ_- will lead to a divergence from this steady state solution and, hence, the state is internally unstable. As regards σ_+ , the result of the internal stability analysis will be just opposite due to the sign change of Δ_{nl} in Eq. (49) and, hence, this state is internally stable, see cases ③ and ④ in Fig. 7. As regards the stability of σ_0 we have analyzed this already in Sec. III and found that if $\Delta^2 > \xi^2$, σ_0 is stable. This inequality is, however, modified slightly here so that it now reads $(\Delta - D)^2 > \xi^2$ because of the shifts from the $\vec{k}_{S,I} + \vec{K}$ waves.

An analysis of internal stability based on numerical calculations was presented in Refs. [23,24] which gave the same result as above. To the best of our knowledge, however, the analytical treatment presented above is the first of its kind.

VII. EXTERNAL STABILITY

In this section we present the external stability analysis of the steady state represented by σ_+ . As σ_- is always internally unstable, this solution is not of any interest. The main idea of our analysis is as follows. We consider the steady state for the two parametric waves found in Sec. V. These two parametric waves will, from now on, be referred to as the primary parametric waves. We then assume that two additional parametric waves, referred to as secondary parametric waves, with small amplitudes and with wave vectors \vec{k}'_S, \vec{k}'_I are present. The new wave vector scheme is shown in Fig. 8. As was the case for the primary parametric waves in Sec. III the wave vectors \vec{k}'_S, \vec{k}'_I can here be chosen arbitrarily as long as the synchronism condition $\vec{k}'_S + \vec{k}'_I = \vec{K}$ is fulfilled. With the external stability analysis we now wish to investigate whether the steady state solution from Sec. V is stable against excitation of any of these secondary parametric waves. If so, the state is said to be externally stable.

To find the increment of instability for the two secondary parametric waves we need again to consider the influence of forced waves. In this particular case we have to include all forced waves generated by the secondary parametric waves and the three steady state waves (with wave vectors \vec{k}_S, \vec{k}_I , and \vec{K}). In total, this involves new forced waves with wave vectors $\vec{k}'_S \pm \vec{k}_S, \vec{k}'_S \pm \vec{k}_I, \vec{k}'_I \pm \vec{k}_S, \vec{k}'_I \pm \vec{k}_I, \vec{k}'_I \pm \vec{K}$, and $\vec{k}'_I \pm \vec{k}'_S$, thus ten forced waves are included. Among these ten waves, however, two are mentioned twice because $\vec{k}'_S - \vec{k}_S$

$= -(\vec{k}'_I - \vec{k}_I)$ and $\vec{k}'_S - \vec{k}_I = -(\vec{k}'_I - \vec{k}_S)$. As a result, eight different forced waves remain to be taken into account. The inclusion of these waves in the theory obviously leads to nonlinear frequency shifts for the secondary parametric waves.

However, in addition to that, another type of contribution is obtained. Consider, for example, the forced wave with wave vector $\vec{k}'_S - \vec{k}_S$. This wave is driven partly by a term proportional to $e_{\vec{k}'_S} e_{\vec{k}_S}^*$ and partly by a term proportional to $e_{\vec{k}_I} e_{\vec{k}'_I}^*$, as $\vec{k}'_S - \vec{k}_S = \vec{k}_I - \vec{k}'_I$. When inserting these terms in the dynamical equation for $e_{\vec{k}'_S}$ two terms proportional to $|e_{\vec{k}_S}|^2 e_{\vec{k}'_S}$ and $e_{\vec{k}_S} e_{\vec{k}_I} e_{\vec{k}'_I}^*$, respectively, appear. The different structure of these two terms is now evident: the first term

gives a nonlinear frequency shift whereas the second one results in a so-called renormalization of the coupling coefficient [22]. Taking all actual nonlinear shifts and renormalizations into account leads to the total nonlinear eigenfrequency and the total coupling coefficient for the secondary \vec{k}'_S wave of the form

$$\begin{aligned} \omega_{\vec{k}'_S}^{\text{nl}} = & \omega_{\vec{k}'_S} + \delta\omega_{\vec{k}'_S, \vec{k}'_S + \vec{k}_S} + \delta\omega_{\vec{k}'_S, \vec{k}'_S - \vec{k}_S} + \delta\omega_{\vec{k}'_S, \vec{k}'_S + \vec{k}_I} \\ & + \delta\omega_{\vec{k}'_S, \vec{k}'_S + \vec{k}_I} + \delta\omega_{\vec{k}'_S, \vec{k}'_S - \vec{k}_I}, \end{aligned} \quad (50)$$

$$h_S^{\text{nl}} = h_{\vec{k}'_S} + \delta h_{\vec{k}'_S; \vec{k}'_S - \vec{k}_S} + \delta h_{\vec{k}'_S; \vec{k}'_S - \vec{k}_I} + \delta h_{\vec{k}'_S; \vec{k}'_S + \vec{k}_I}.$$

The individual frequency shifts can be found using Eq. (32) and the corrections to the coupling coefficient are given by

$$\begin{aligned} \delta h_{\vec{k}'_S; \vec{k}'_S - \vec{k}_S} &= \frac{V_{\vec{k}'_S; \vec{k}_S, \vec{k}_I - \vec{k}'_I}(\omega_{\vec{k}_S}, \omega_{\vec{k}_I} - \omega_{\vec{k}'_I}) V_{\vec{k}_I - \vec{k}'_I; -\vec{k}'_I, \vec{k}_I}(-\omega_{\vec{k}'_I}, \omega_{\vec{k}_I})}{\omega_{\vec{k}_I - \vec{k}'_I} + \omega_{\vec{k}'_I} - \omega_{\vec{k}_I}} \sigma \equiv S_{\vec{k}'_S, \vec{k}'_S - \vec{k}_S} \sigma, \\ \delta h_{\vec{k}'_S; \vec{k}'_S - \vec{k}_I} &= \frac{V_{\vec{k}'_S; \vec{k}_I, \vec{k}_S - \vec{k}'_I}(\omega_{\vec{k}_I}, \omega_{\vec{k}_S} - \omega_{\vec{k}'_I}) V_{\vec{k}_S - \vec{k}'_I; -\vec{k}'_I, \vec{k}_S}(-\omega_{\vec{k}'_I}, \omega_{\vec{k}_S})}{\omega_{\vec{k}_S - \vec{k}'_I} + \omega_{\vec{k}'_I} - \omega_{\vec{k}_S}} \sigma \equiv S_{\vec{k}'_S, \vec{k}'_S - \vec{k}_I} \sigma, \\ \delta h_{\vec{k}'_S; \vec{k}'_S + \vec{k}_I} &= \frac{V_{\vec{k}'_S; -\vec{k}'_I, \vec{k}}(-\omega_{\vec{k}_I}, \Omega) V_{\vec{k}; \vec{k}_I, \vec{k}_S}(\omega_{\vec{k}_I}, \omega_{\vec{k}_S})}{\omega_{\vec{k}} - \Omega} \sigma \equiv S_{\vec{k}'_S, \vec{k}'_S + \vec{k}_I} \sigma. \end{aligned} \quad (51)$$

The explicit expressions for the S coefficients are evident from Eq. (51). The first two terms are due to the difference waves with wave vectors $\vec{k}'_S - \vec{k}_S$ and $\vec{k}'_S - \vec{k}_I$ whereas the last term is due to the feedback from the two primary parametric waves on the pump wave. Note that the coupling coefficients are no longer real because the corrections from Eq. (51) are proportional to the complex parameter σ .

After having found the modified eigenfrequencies and coupling coefficients for the pair of secondary parametric waves [the eigenfrequency and coupling coefficient for the \vec{k}'_I wave may be found by interchanging the indices S and I in Eq. (50)] we obtain two coupled amplitude equations for the secondary parametric waves that are similar in form to Eqs. (34) and (35):

$$\dot{e}_{\vec{k}'_S} + [\gamma + i(\omega_{\vec{k}'_S}^{\text{nl}} - \omega'_S)] e_{\vec{k}'_S} = -i h_{\vec{k}'_S}^{\text{nl}} e_{\vec{k}'_I}^*, \quad (52)$$

$$\dot{e}_{\vec{k}'_I}^* + [\gamma - i(\omega_{\vec{k}'_I}^{\text{nl}} - \omega'_I)] e_{\vec{k}'_I}^* = i h_{\vec{k}'_I}^{\text{nl}} e_{\vec{k}'_S}. \quad (53)$$

Again, the solution to this linear set of equations may be taken in the form $e_{\vec{k}'_S}, e_{\vec{k}'_I}^* \propto \exp(\nu t)$. As a result, we get from the real and imaginary parts of the characteristic equation

$$2(\gamma + \nu) \Delta_{\text{nl}}^- = \text{Im}\{h_{\vec{k}'_S}^{\text{nl}}(h_{\vec{k}'_I}^{\text{nl}})^*\}, \quad (54)$$

$$(\gamma + \nu)^2 + (\Delta_{\text{nl}}')^2 - (\Delta_{\text{nl}}^-)^2 = \text{Re}\{h_{\vec{k}'_S}^{\text{nl}}(h_{\vec{k}'_I}^{\text{nl}})^*\},$$

where $\text{Re}\{\}$ and $\text{Im}\{\}$ stand for the real and imaginary parts and

$$\Delta_{\text{nl}}' = \frac{1}{2}(\Omega - \omega_{\vec{k}'_S}^{\text{nl}} - \omega_{\vec{k}'_I}^{\text{nl}}), \quad (55)$$

$$\Delta_{\text{nl}}^- = \frac{1}{2}(\omega'_I - \omega'_S + \omega_{\vec{k}'_S}^{\text{nl}} - \omega_{\vec{k}'_I}^{\text{nl}}).$$

The condition of external stability reads $\nu < 0$. By combining Eqs. (54) we find that the nonlinear stationary state is externally stable against excitation of secondary parametric waves with wave vectors \vec{k}'_S and \vec{k}'_I if the inequality

$$\gamma^2 + (\Delta_{\text{nl}}')^2 - \text{Re}\{h_{\vec{k}'_S}^{\text{nl}}(h_{\vec{k}'_I}^{\text{nl}})^*\} - \left(\frac{\text{Im}\{h_{\vec{k}'_S}^{\text{nl}}(h_{\vec{k}'_I}^{\text{nl}})^*\}}{2\gamma}\right)^2 \geq 0 \quad (56)$$

is fulfilled. The equal sign gives the threshold of the external instability.

Let us consider Eq. (56) for the particular case of transversal parametric oscillation, $X=0$, and let the wave vectors \vec{k}'_S and \vec{k}'_I be represented by $(K/2)[(1-X')\hat{x} + Y'\hat{y}]$ and $(K/2)[(1+X')\hat{x} - Y'\hat{y}]$, respectively. If we assume that $\varepsilon = 0.25$ and Y, X', Y' are all much smaller than unity, it is possible to obtain the following simplified expressions for the parameters involved in Eq. (56):

$$\frac{\Delta'_{nl}}{\omega_{\vec{K}/2}} \cong -\frac{5}{72} m^2 - X'^2 - \frac{1}{10} \left(-\frac{5}{72} m^2 + \frac{\xi}{\omega_{\vec{K}/2}} \right) \left(\frac{40}{3} - \frac{4X'^2}{X'^2 + (Y-Y')^2} - \frac{4X'^2}{X'^2 + (Y+Y')^2} \right),$$

$$\frac{h'_{S'}}{\omega_{\vec{K}/2}} \cong -\frac{m}{3} (1-X') + \left(\frac{10}{3} + 4X' - \frac{X'[2X' - (Y-Y')^2]}{X'^2 + (Y-Y')^2} - \frac{X'[2X' - (Y+Y')^2]}{X'^2 + (Y+Y')^2} \right) \sigma_+,$$

$$\frac{h'_{I'}}{\omega_{\vec{K}/2}} \cong -\frac{m}{3} (1+X') + \left(\frac{10}{3} - 4X' - \frac{X'[2X' + (Y-Y')^2]}{X'^2 + (Y-Y')^2} - \frac{X'[2X' + (Y+Y')^2]}{X'^2 + (Y+Y')^2} \right) \sigma_+, \quad (57)$$

$$\sigma_+ \cong \frac{3}{5} m \left(-\frac{5}{72} m^2 + \frac{\xi}{\omega_{\vec{K}/2}} \right) \left(\frac{\xi}{\omega_{\vec{K}/2}} + iQ_{\vec{K}/2}^{-1} \right),$$

$$\frac{\xi}{\omega_{\vec{K}/2}} \cong \left(-Q_{\vec{K}/2}^{-2} + \frac{m^2}{9} \right)^{1/2}.$$

Consider now some value of Y , i.e., some degree of transversal split between the primary parametric wave vectors. To work out whether the stationary state for this particular case is externally stable or not, we need to find the minimum of the left-hand side of the inequality (56). If, at this minimum, the left-hand side is negative, the stationary state is unstable; if it is positive, it is stable. By using the expressions in Eqs. (57) with $Q_{\vec{K}/2} = 6.5$ and $m = 1$ one can produce contour plots of the left-hand side for different values of Y . A series of these plots is shown in Fig. 9. The symmetries with respect to the X' and Y' axes means that we need only comment on the quadrant where X' and Y' are positive. Starting at $Y = 0.01$ one can see that the minimum of the left-hand side appears at $X' \cong 0.07$ and $Y' = 0$ and that at this minimum the left-hand side $\cong -0.06$. Thus for $Y = 0.01$ the stationary state is externally unstable against growth of secondary parametric waves with wave vectors $\vec{k}_{S,I} = (K/2)(1 \pm 0.07)\hat{x}$. This type of instability may be referred to as longitudinal instability as the secondary parametric wave vectors are parallel with \vec{K} . This is opposed to the modulational instability found for the $\vec{K}/2$ subharmonic case [22]. At $Y = 0.10$ the stationary state is still longitudinally unstable but the minimum has moved further out the X' axis and, moreover, the minimum has increased to -0.003 . It means that the stationary state is still unstable but the instability is very weak as the minimum is close to zero. Moreover, the region in X' - Y' space in which secondary parametric waves can be excited is drastically reduced, see the dashed contour. At $Y = 0.12$ the stationary state has become stable as the minimum, which still appears on the X' axis, is positive. At $Y = 0.14$ the minimum has moved away from the X' axis but it is even more positive, so the stationary state stabilizes further as Y is increased. Finally, at $Y = 0.18$ the minimum has moved close to the Y' axis.

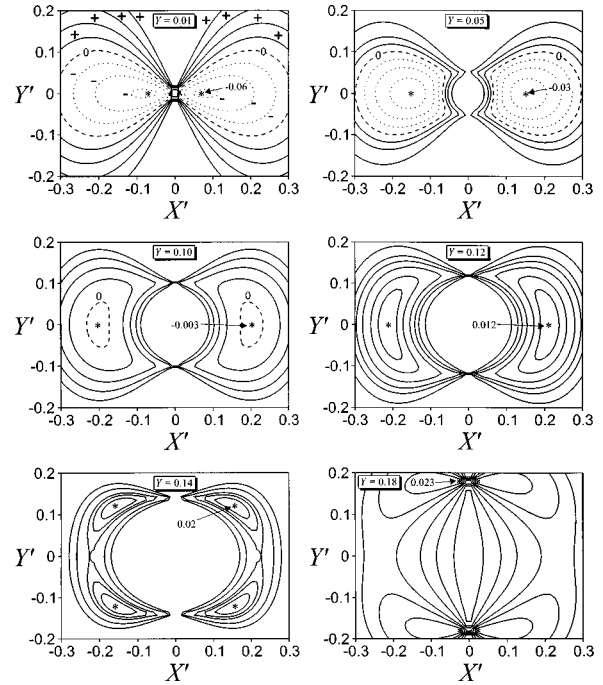


FIG. 9. Contour plots of the left-hand side of inequality (56) in the X' - Y' plane for six different values of Y . The dotted contours represent negative values of the left-hand side, the dashed line represent the threshold left-hand side equal to 0, and the solid lines represent positive values of the left-hand side. In all six plots the minima are marked by an asterisk, *. The minimum values given in the plot have been normalized by $\omega_{\vec{K}/2}$.

As mentioned, the contour plots in Fig. 9 are based on the simplified expressions in Eqs. (57). To obtain accurate results for a larger region of Y we have used the exact formulas for Δ'_{nl} , $h'_{S'}$, and $h'_{I'}$. These results are shown in Fig. 10 where the minimum is traced through the X' - Y' space for increasing Y . It is seen that there is a good agreement with Fig. 9. The numerical point of stabilization is at $Y = 0.09$ which is only slightly lower than what was found from the

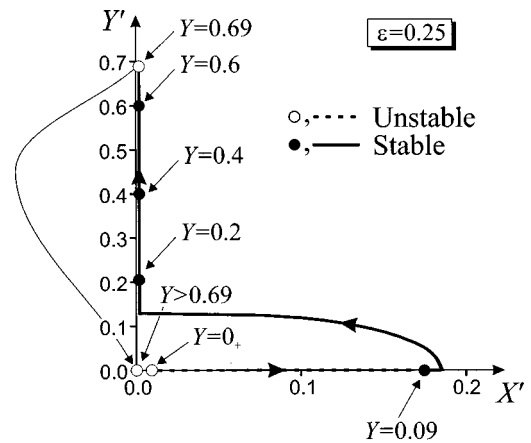


FIG. 10. The points of (X', Y') that give a minimum left-hand side of Eq. (56), for different values of Y . These results are obtained from the exact formula. The open circles and dashed lines notify unstable points or branches; the closed circles and solid lines notify stable points or branches. At $Y = 0.69$ the minimum jumps from $(0_+, 0.69)$ to $(0, 0)$.

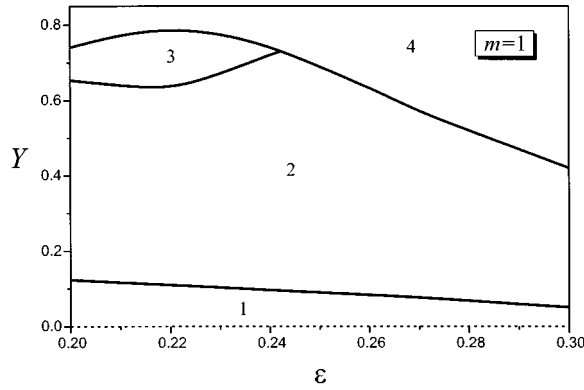


FIG. 11. Diagram of the different regions of stability or instability for transversal parametric oscillation at $m=1$. The dashed abscissa axis indicates that the stationary state is modulationally unstable for $Y=0$. In region 1 we have longitudinal instability, in region 2 the stationary state is stable, in region 3 we have modulational instability, and in region 4 we have instability against excitation of the $\vec{K}/2$ subharmonic wave.

simple expressions. The stationary state is stable until $Y=0.69$ where the state becomes unstable against excitation of the $\vec{K}/2$ subharmonic wave, hence another nonmodulational instability appears. In total, one can conclude that for $\varepsilon=0.25$ and $m=1$ the state of transversal parametric oscillation is stable for a certain degree of transversal split between the wave vectors of the primary parametric waves. It is worth noting that what is causing the instability are the shifts from the difference waves with wave vectors $\vec{k}'_S - \vec{k}_{S,I}$, $\vec{k}'_I - \vec{k}_{S,I}$. In the absence of these forced waves the stationary state would have been stable.

By performing similar analyses for other values of ε it is possible to work out the region of stability of transversal parametric oscillation in the ε - Y plane, see Fig. 11. It is seen that with increasing ε , from 0.2 to 0.3, the minimum “stable value” of Y decreases almost linearly from 0.12 to 0.05. From above the stable region is bounded by the two regions, (3) and (4). In region (3) the stationary state is modulationally unstable, i.e., secondary waves with wave vectors near \vec{k}'_S and \vec{k}'_I are excited here. In region (4) the stationary state is unstable against excitation of the $\vec{K}/2$ subharmonic wave.

Figures 12 and 13 show similar diagrams for $m=0.7$ and

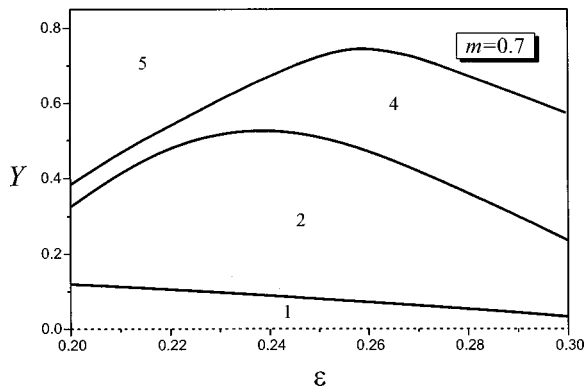


FIG. 12. Same as Fig. 11, except that $m=0.7$. In region 5 the stationary solution σ_+ is nonexistent.

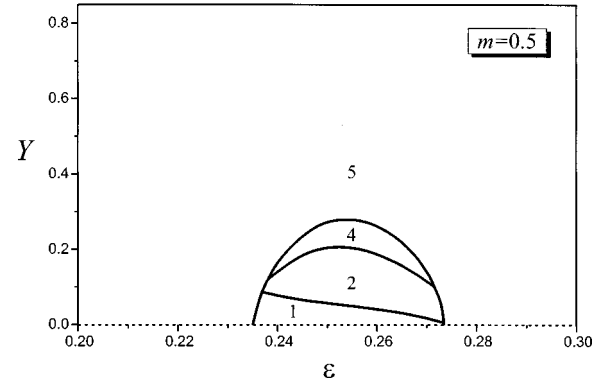


FIG. 13. Same as Fig. 12, except that $m=0.5$.

0.5. It is seen that the stable region (2) shrinks drastically as m is decreased. At $m \approx 0.46$ the regions (1), (2), and (4) disappear, meaning that the solution σ_+ no longer exists.

VIII. DISCUSSION

In the present paper we have found the stationary states of transversal parametric oscillation and analyzed the stability above threshold of the parametric waves' excitation. We have shown that the growth of the primary parametric waves is stabilized due to formation of nonlinearly forced waves that exert a feedback on the parametric waves. This feedback can be represented as a nonlinear shift of the eigenfrequencies of the parametric waves. Thus the stabilization is working by pushing the parametric waves away from resonance. We have analyzed to which extent this stationary state is stable against excitation of secondary pairs of parametric waves. Our analysis is restricted to the case of transversal parametric oscillation in which the primary parametric wave vectors have equal longitudinal components.

The outcome of the stability analysis depends, of course, upon the parameters of a particular crystal as well as on the experimental conditions. However, a considerable part of these parameters enter the formulas via the quality factor $Q_{\vec{K}/2}$ of the wave with wave vector $\vec{K}/2$. Apart from this quality factor we have only the intensity contrast m and the temporal frequency of the light pattern, Ω , to take care of. The optimum conditions for excitation of parametric waves are fulfilled if $\Omega \approx 4\omega_{\vec{K}}$ and $m=1$. In this case we have found that for $0.09 < |Y| < 0.69$, where Y is the ratio of the transversal to the longitudinal component of the parametric wave vectors, the stationary state is stable. Outside this interval the stationary state, in particular the $\vec{K}/2$ subharmonic state, is unstable. Conclusively, we have succeeded in finding the first stable parametric waves. The region of Y , in which the stationary state is stable, shrinks drastically as m is decreased. At $m=0.46$ the region of stability disappears.

We found different types of instability. For the $\vec{K}/2$ subharmonic case the state is unstable against excitation of waves near to $\vec{K}/2$; this is referred to as modulational instability. Then, for a small transversal split between the parametric wave vectors we find that the stationary state is unstable against excitation of parametric waves with longitudinal wave vectors. On the other hand, if the transversal split is too large, then, depending on ε , the state becomes

either modulationally unstable or it becomes unstable against excitation of a $K/2$ subharmonic wave.

It is essential in the stability analysis to include also waves that are generated by quadratic, nonlinear interactions between the secondary parametric waves and the primary, stationary waves. These waves are referred to as forced waves and they can be included in the analysis in an extraordinarily simple way, in the sense that they can be represented either as nonlinear shifts of the eigenfrequencies of the secondary parametric waves or as renormalizations of the coupling constant between the secondary parametric waves. In this manner, it is possible to include all the forced waves and still keep the simple structure of the amplitude equations.

One might now ask the question: What kind of predictions can be made as regards the outcome of a two-wave mixing (running grating) experiment performed in a sillenite crystal? First of all, we know that (for certain parameters) the fundamental wave is unstable against excitation of parametric waves with wave vectors near $\vec{K}/2$. But what happens in steady state is still a bit of an open question. We know that a single $\vec{K}/2$ subharmonic wave cannot be the final state, as it is unstable. On the other hand, we also know that the $\vec{K}/2$ subharmonic wave has the largest increment as compared to transversal parametric waves, hence the buildup of a $\vec{K}/2$

subharmonic is favored. What might happen is that when the $\vec{K}/2$ subharmonic wave amplitude has grown up to some level a broadening process starts which stabilizes the instability. If this is the case, the transversal parametric oscillation state will never arise. Another possibility is that instead of a broadening of the $\vec{K}/2$ subharmonic wave, a pair of growing transversal parametric waves will take over and stabilize the instability. In this case transversal parametric oscillation becomes the final state.

One way to experimentally verify the existence of stable transversal parametric waves would be to use the so-called PPA technique [30] in which a second interference pattern excites the parametric waves. Then, after the transversal waves have grown up the second intensity pattern can be removed after which the parametric waves should keep being present without any broadening. The results of such an experiment would be highly interesting.

ACKNOWLEDGMENTS

E.V.P., H.C.P., and P.M.J. were supported by Danish Natural Science Research Council Grant Nos. 9502764 and 9600986. B.I.S. wishes to acknowledge support from the Russian Foundation for Fundamental Research, Grant No. 96-02-19126.

-
- [1] F. Chen, *Introduction to Plasma Physics and Controlled Fusion*, 2nd ed. (Plenum, New York, 1984).
 - [2] V. E. Zakharov, V. S. L'vov, and G. Fal'kovich, in *Kolmogorov Spectra of Turbulence: Wave Turbulence*, Springer Series in Nonlinear Dynamics (Springer-Verlag, Berlin, 1992).
 - [3] V. S. L'vov, in *Wave Turbulence under Parametric Excitation. Application to Magnets*, Springer Series in Nonlinear Dynamics (Springer-Verlag, Berlin, 1994).
 - [4] Y. R. Shen, *The Principles of Nonlinear Optics* (Wiley, New York, 1984).
 - [5] Ph. Refregier, L. Solymar, H. Rajbenbach, and J.-P. Huignard, *J. Appl. Phys.* **58**, 45 (1985).
 - [6] S. Mallick, B. Imbert, H. Ducollet, J.-P. Herriau, and J. P. Huignard, *J. Appl. Phys.* **63**, 5660 (1988).
 - [7] H. C. Pedersen and P. M. Johansen, *J. Opt. Soc. Am. B* **12**, 1065 (1995).
 - [8] H. C. Pedersen and P. M. Johansen, *Opt. Lett.* **19**, 1418 (1994).
 - [9] J. Takacs and L. Solymar (private communication).
 - [10] H. C. Pedersen and P. M. Johansen, *Phys. Rev. Lett.* **77**, 3106 (1996).
 - [11] B. I. Sturman, M. Mann, J. Otten, and K. H. Ringhofer, *J. Opt. Soc. Am. B* **10**, 1919 (1993).
 - [12] T. E. McClelland, D. J. Webb, B. I. Sturman, and K. H. Ringhofer, *Phys. Rev. Lett.* **73**, 3082 (1994).
 - [13] B. I. Sturman, T. E. McClelland, D. J. Webb, E. Shamonina, and K. H. Ringhofer, *J. Opt. Soc. Am. B* **12**, 1621 (1995).
 - [14] R. F. Kazarinov, R. A. Suris, and B. I. Fuks, *Fiz. Tekh. Poluprovodn.* **6**, 572 (1972) [*Sov. Phys. Semicond.* **6**, 500 (1972)].
 - [15] S. I. Stepanov, V. V. Kulikov, and M. P. Petrov, *Opt. Commun.* **44**, 19 (1982).
 - [16] D. J. Webb, L. B. Au, D. C. Jones, and L. Solymar, *Appl. Phys. Lett.* **57**, 1602 (1990).
 - [17] D. J. Webb and L. Solymar, *Opt. Commun.* **74**, 386 (1990).
 - [18] I. Richter, A. Grunnet-Jepsen, J. Takacs, and L. Solymar, *IEEE J. Quantum Electron.* **30**, 1645 (1994).
 - [19] J. Takacs and L. Solymar, *Opt. Lett.* **17**, 247 (1992).
 - [20] H. C. Pedersen and P. M. Johansen *J. Opt. Soc. Am. B* (to be published).
 - [21] B. I. Sturman, M. Aguilar, and F. Agullo-Lopez, *Phys. Rev. B* **54**, 13 737 (1996).
 - [22] B. I. Sturman, M. Aguilar, F. Agullo-Lopez, and K. H. Ringhofer, *Phys. Rev. E* **55**, 6072 (1997).
 - [23] B. I. Sturman, A. Bledowski, J. Otten, and K. H. Ringhofer, *J. Opt. Soc. Am. B* **9**, 672 (1992).
 - [24] A. Bledowski, J. Otten, K. H. Ringhofer, and B. Sturman, *Zh. Eksp. Toer. Fiz.* **102**, 406 (1992) [*Sov. Phys. JETP* **75**, 215 (1992)].
 - [25] N. V. Kukhtarev, V. B. Markov, S. G. Odulov, M. S. Soskin, and V. L. Vinetskii, *Ferroelectrics* **22**, 949 (1979).
 - [26] T. J. Hall, R. Laura, L. M. Connors, and P. D. Foote, *Prog. Quantum Electron.* **10**, 77 (1985).
 - [27] P. M. Johansen, *J. Phys. D* **22**, 247 (1989).
 - [28] T. E. McClelland, D. J. Webb, B. I. Sturman, E. Shamonina, M. Mann, and K. H. Ringhofer, *Opt. Commun.* **131**, 315 (1996).
 - [29] T. E. McClelland, D. J. Webb, B. I. Sturman, M. Mann, and K. H. Ringhofer, *Opt. Commun.* **113**, 371 (1995).
 - [30] H. C. Pedersen and P. M. Johansen, *Phys. Rev. Lett.* **76**, 4159 (1996).